Pyrgeometer Data Reduction and Calibration Procedures

By
B. Albrecht and S.K. Cox

Department of Atmospheric Science
Colorado State University
Fort Collins, Colorado

March 1976

Colorado State University

Department of Atmospheric Science

Paper No. 251

PYRGEOMETER DATA REDUCTION
AND
CALIBRATION PROCEDURES

By

B. Albrecht and S. K. Cox

Department of Atmospheric Science

Colorado State University

Fort Collins, Colorado

80523

May 1976

Atmospheric Science Paper No. 251

TABLE OF CONTENTS

ABSTRACT

The actual performance of an Eppley pyrgeometer is compared to the desired theoretical performance. Several systematic errors are identified and evaluated in detail. The three most significant errors identified are due to (1) battery voltage uncertainties (2) non-linearity of circuitry at extreme temperature and (3) differential heating of the instrument. The elimination of the error due to differential heating is found to be essential to the successful calibration of the instrument. A pyrgeometer laboratory calibration technique is described.

Pyrgeometer measurements made from aircraft are shown to have potential errors as large as 50 Wm^{-2}. These errors, however, do not significantly affect the net radiation provided the upward and downward facing pyrgeometers are at the same equilibrium temperature, and may be largely eliminated by making accurate temperature measurements of the KRS-5 dome and the cold junctions of the thermopile. The corrections considered in this paper not only reduce the absolute errors but significantly decrease the transient response of the instrument. The feasibility of using an empirical expression to correct errors due to solar heating is also demonstrated for aircraft measurements.

LIST OF TABLES

LIST OF FIGURES

LIST OF FIGURES

I. Introduction

The availability of a moderately priced thermopile instrument which could isolate the infrared (4-50 μm) portion of the spectrum has made it possible to directly measure hemispheric infrared irradiances. Heretofore, most broadband infrared irradiance observations were deduced from a total (solar and infrared) irradiance measurement and an independent solar irradiance measurement by differencing the two values.

The Eppley Laboratory's pyrgeometer is an instrument designed to measure hemispheric radiation in the 4-50 μm spectral range. The development of this instrument was first described by Drummond, et al (1970). Prior to GATE, (GARP Atlantic Tropical Experiment), the performance of this instrument was evaluated to determine the feasibility of using this instrument to make broadband measurements of longwave radiation from aircraft. The results of this evaluation and the theory of operation of the Eppley pyrgeometer were reported by Albrecht, et al (1974) (abbreviated A74). Similar instruments have been described by G.P. Faraponova (1966), G.P. Faraponova and R.G. Timanovskaya (1966) and Kozyrev (1966).

Theoretically, the pyrgeometer instrument should yield accurate (5%) measurements of the infrared irradiance. However, a number of problems have been encountered by users since the introduction of this instrument. It is the purpose of this paper to report both problems and suggested solutions to these problems so that the scientific community may take advantage of the opportunity to measure broadband infrared irradiances directly.

The results given by A74 indicate that under certain circumstances, pyrgeometer measurements made from aircraft may be more precise than

those made from a ground station installation. This is particularly true for daytime measurements when the solar load on the sensor is large. In the ground station installation, the hemispheric filter of the instrument is heated by the solar radiation which may result in erroneously high outputs (Enz et al 1975). When mounted on an aircraft, the increased air flow tends to minimize the effect of the solar heating.

In other instances, however, the extreme temperature variations experienced by sensors mounted on aircraft may seriously degrade the accuracy of the pyrgeometer measurements. This is particularly true for low temperature applications of the sensors such as aircraft observations at very high altitudes. Furthermore, for slow moving aircraft or surface observations, airflow over the instrument may not be sufficient to completely eliminate the solar heating effect.

In this paper the theory of operation of the pyrgeometer is reviewed briefly in order to enumerate the systematic errors and pitfalls which may be encountered when calibrating or making measurements with the pyrgeometer. Various techniques for correcting these errors are explored. These techniques are illustrated by correcting sample data sets obtained from aircraft measurements made during GATE.

While airbrone measurements were the authors' principal concern during the preparation of this report, the results and techriques are equally applicable to ground based pyrgeometer measurements. It is the authors' belief that incorporation of the techniques recommended in this paper will result in much higher quality pyrgeometer data for both airborne and surface applications.

II. Pyrgeometer Performance: Theoretical vs Actual

The Eppley pyrgeometer consists of a thermopile shielded by a KRS-5 hemisphere. A schematic of the pyrgeometer is shown in Figure 1. The thermopile is coated with flat black paint which has a spectral response to incident radiation that is uniform from 3-50 μm. An interference filter is vacuum deposited on the inside of the KRS-5 hemisphere to prevent the transmission of radiation at wavelengths less than 3.5 μm. The spectral transmissivity of the KRS-5 hemisphere and the interference filter is given in A74 (see Appendix A).

In theory the radiation incident upon the pyrgeometer may be determined by accurately specifying the heat budget of the thermopile and the KRS-5 filter. By considering such a budget, the incident radiation may be shown to be a function of the thermopile output, the thermopile cold junction temperatures, and the temperature of the hemispheric filter. The heat budget for the Eppley instrument may be written

$$L = E(c_1 + c_2 T_s^3) + \varepsilon_o \sigma T_s^4 - k\sigma(T_d^4 - T_s^4) \qquad (1)$$

where L is the incident irradiance, E is the thermopile output, T_s is the temperature of the thermopile cold junctions (referred to as the sink temperature) and T_d is the temperature of the KRS-5 hemisphere; ε_o is the emissivity of the thermopile surface, σ is the Stefan-Boltzman constant and k, c_1 and c_2 are constants which may be determined during calibration of the instrument. A detailed derivation of (1) is given in Appendix A.

In practice, thermistor-resistor networks are used in the Eppley pyrgeometer to account for the T_s^3 and T_s^4 dependencies indicated in Eq. (1). The constants c_1, c_2, and ε_o are determined implicitly during the manufacturer's calibration. During these calibrations, the

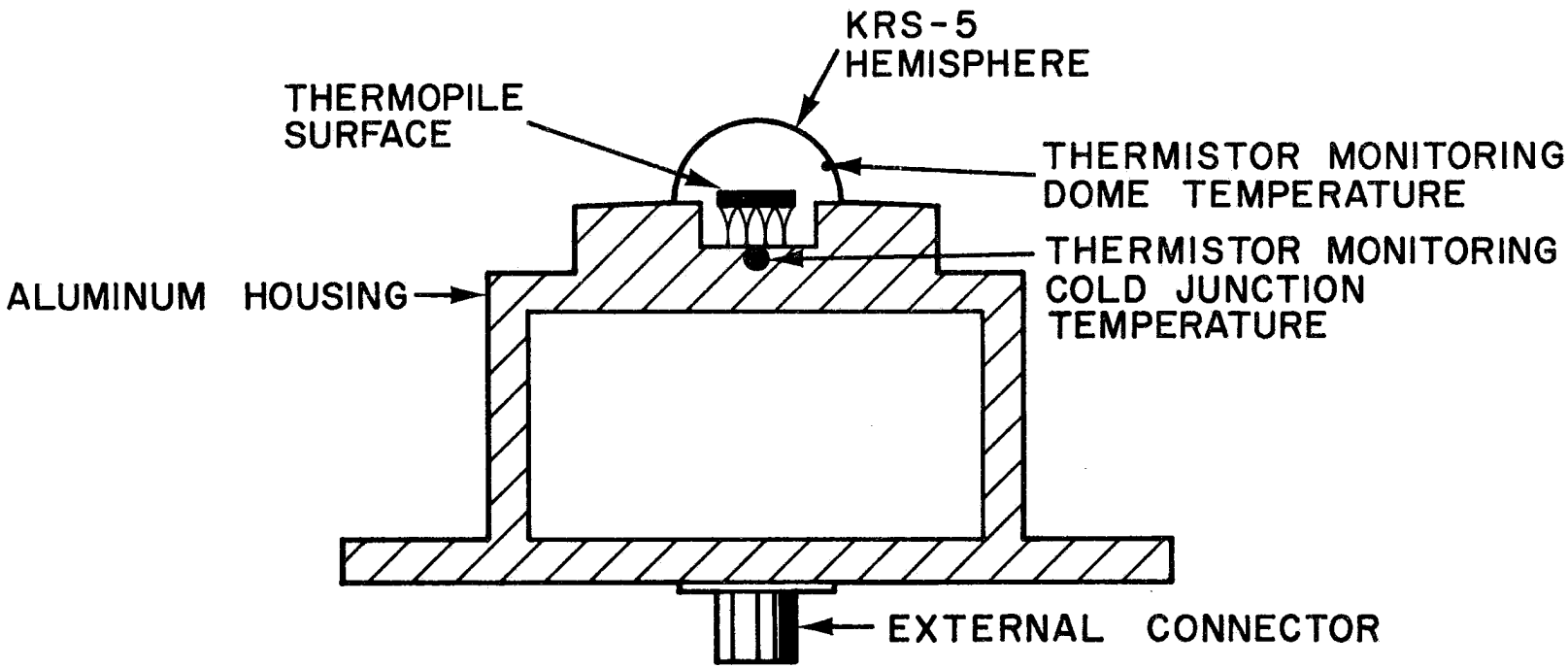

Figure 1. Sketch of the Eppley pyrgeometer (not to scale).

instrument is maintained so that $T_d = T_s$; hence, the last term in Eq. (1) is not considered. In actual operation, however, nothing guarantees that T_d will equal T_s.

The internal pyrgeometer circuitry used to represent the temperature dependencies in the first two terms of Eq. (1) is shown in Fig. 2. The right hand side of this circuit is the temperature compensated thermopile output and represents $E(c_1 + c_2 T_s^3)$ in Eq. (1). The left hand side of the circuit approximates the blackbody emission of the thermopile surface and represents $\varepsilon_o \sigma T_s^4$ in Eq. (1). The emf source, E_A, indicated in this portion of the circuit is supplied by a small mercury cell that is mounted within the instrument.

Obviously, it may be difficult, if not impossible, to design a simple circuit such as that shown in Fig. 2 which would give a perfect representation of the temperature dependencies indicated in Eq. (1). In some cases, the deficiencies of the thermistor-resistor networks may not be significant. For example, in Eq. (1) $c_1 + c_2 T_s^3$ represents the sensitivity of the thermopile. For all temperatures $c_1 >> c_2 T_s^3$ and $E(c_1 + c_2 T_s^3)$ is typically 3 or 4 times smaller (in absolute value) than $\varepsilon_o \sigma T_s^4$ in Eq. (1). Consequently, errors in the electrically compensated thermopile output may not contribute significantly to errors in the measured irradiance value. Errors in the instrument equivalent of the $\varepsilon_o \sigma T_s^4$ term, however, may be significant.

There are at least two possible circumstances when the left-hand side of the circuit shown in Fig. 2 does not accurately produce a signal equivalent to the $\varepsilon_o \sigma T_s^4$ term. The first is due to uncertainties in the battery voltage E_A. The second is the inability of the circuit to reproduce the T_s^4 dependence over a large range of temperatures.

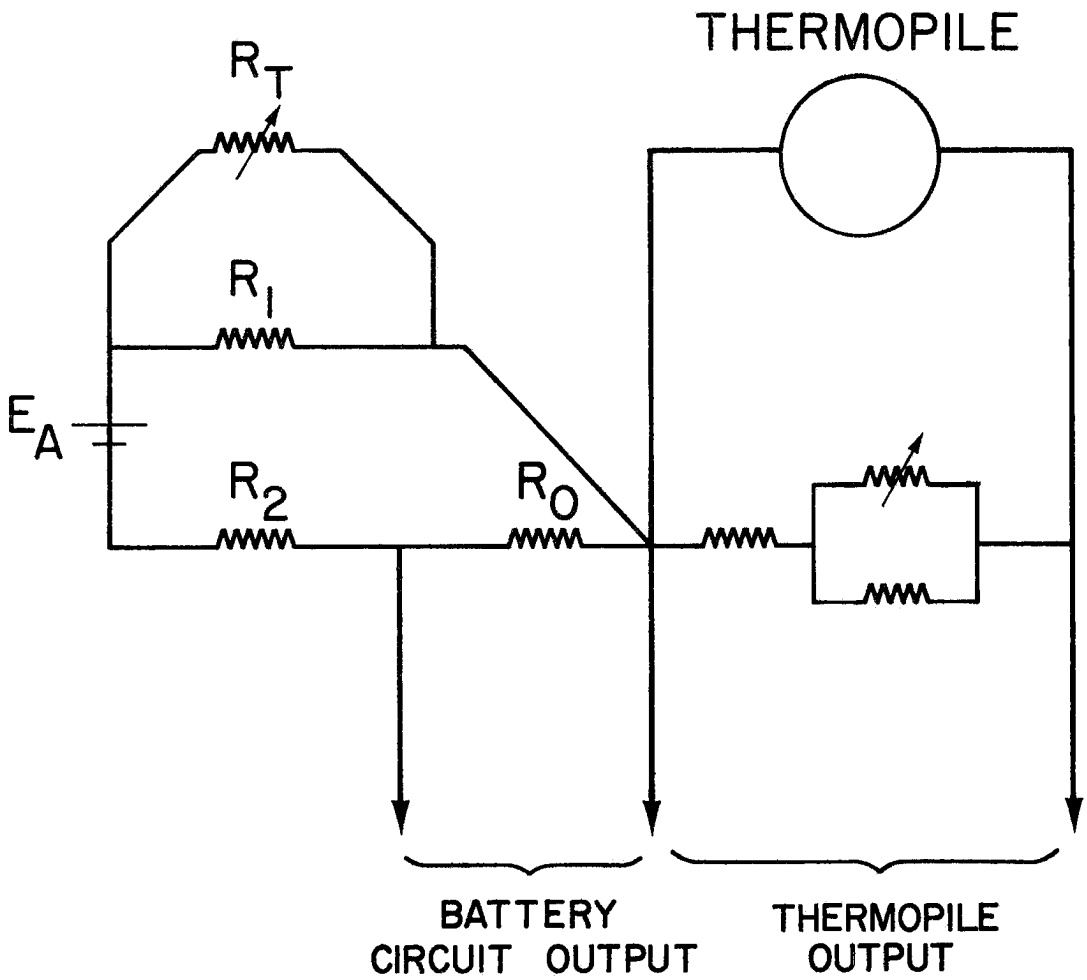

TYPICAL RESISTANCE VALUES

R_T = 10 KΩ @ 25°C

R_1 = 35.8 KΩ

R_2 = 9.97 KΩ

R_0 = 35.4 KΩ

$\frac{1}{n}$ = 166.9 $Wm^{-2}mv^{-1}$

Figure 2 . Schematic of the pyrgeometer circuit.

As indicated above, the Eppley pyrgeometer circuitry does not account for the $k\sigma(T_d^4 - T_s^4)$ term which appears in Eq. (1). The numerical value of k may vary between instruments and may be as large as $\sqrt{4}$. This implies that an uncertainty of .1°C between the temperature difference of the dome and sink will result in an uncertainty of 3-4 Wm^{-2}. in the indicated irradiance. For ground based measurements, the solar heating of the dome may easily produce a 10°C difference between the temperature of the filter and the cold junctions. When mounted on an aircraft, the increased air flow over the instrument tends to decrease the solar heating effect. However, for slow moving aircraft which fly with a large angle of attack, the solar heating may still be significant. Enz, et al (1975) attempted to use a ventilation system to decrease the solar heating effect for ground-based measurements.

The $k\sigma(T_d^4 - T_s^4)$ term may also be significant for other conditions encountered on aircraft flights. For example, immediately after an ascent or descent to a different level in the atmosphere, the KRS-5 hemisphere responds quickly to the resulting change in temperature. The instrument housing (containing the thermopile cold junctions), however, responds much more slowly because of its large thermal mass. Even after several minutes of flight at a level where the temperature is constant, compressional heating of the instrument may maintain the dome and sink of the instrument at slightly different temperatures.

To summarize the possible errors described above, Eq. (1) may be written as:

$$L = L_I + \delta L_B + \delta L_T + \delta L_{DS} \qquad (2)$$

where L_I is the uncorrected instrument output, L_B is a correction for differences between the actual battery voltage, E_A, and some standard

voltage E_o. The δL_T term in Eq. (2) is a correction for the non-linearity between the battery circuit output L_o and $\varepsilon_o \sigma T_s^4$; δL_{DS} represents the $-k\sigma(T_d^4 - T_s^4)$ in Eq. (1). Each of these correction terms will be considered in detail in the following sections.

III. Pyrgeometer Calibration

In the procedure described below Eppley pyrgeometers are calibrated by using a conical cavity blackbody of large thermal mass. Various target temperatures are obtained by cooling the blackbody to approximately -10°C and allowing the blackbody to warm as the calibrations are performed. Blackbody temperatures are measured at several points on the surface of the conical aperture using thermocouples attached to this surface. Temperature differences between these points are less than .2°C.

Calibration of the Eppley pyrgeometer, however, requires some special care due in particular to the dome-sink temperature difference term in Eq. (1). If, for example, the instrument is faced into a conventional blackbody target, the filter temperature will increase with time if the target is initially warmer than the instrument. The housing of the instrument may also change with time but at a much slower rate. Consequently, the $k\sigma(T_d^4 - T_s^4)$ term may be significant. An example of a calibration procedure which properly accounts for this effect is given below.

To determine the sensitivity of the Eppley thermopile, the instrument is faced into the blackbody cavity while thermopile output, sink temperature and dome temperature are recorded as a function of time. In the results given here the dome temperature is determined by a single bead thermistor attached to the inside of the KRS-5 hemisphere. The sink temperature is determined by a thermistor attached to the housing as close to the cold junctions as possible (c.f. Fig. 1). An example of instrument output and the dome and sink temperatures as a function of time is shown in Fig. 3 for a single calibration point. Initially, the KRS-5

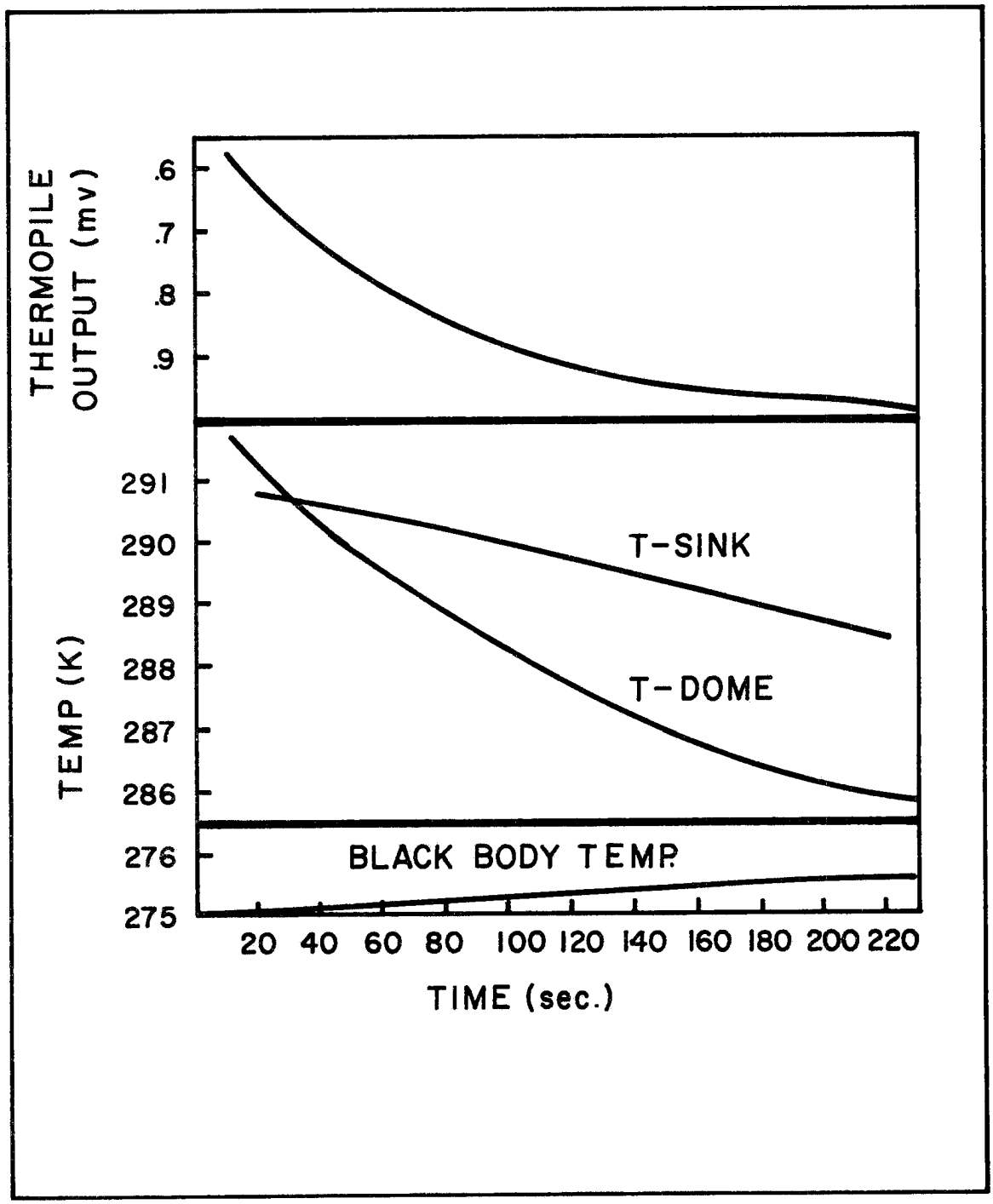

Figure 3. Variation of thermopile output and dome and sink pyrgeometer temperatures as a function of time during a black body calibration.

dome was warmer than the sink, however, when the instrument was faced into the blackbody, the dome cooled quickly as it lost energy to the cold blackbody; at the same time the thermopile sink cooled much more slowly since its thermal mass is much greater. After approximately three minutes the dome and sink cooled at approximately the same rate. During this time, the instrument output initially decreased rapidly and then stabilized after approximately three minutes. This behavior is consistent with Eq. (1) which may be written in the form

$$\frac{E}{\eta} = L - \varepsilon_0 \sigma T_s^4 + k\sigma(T_d^4 - T_s^4) \qquad (3)$$

where $\frac{1}{\eta}$ is the instrument sensitivity, $(c_1 + c_2 T_s^3)$. The dominance of the $k\ (T_d^4 - T_s^4)$ is apparent in the variation of output as a function of time as shown in Fig. 3 since initially L and T_s vary only slowly.

To determine $\frac{1}{\eta}$ in Eq. (3), the instrument output, E, at points where $T_d = T_s$ is plotted against $L - \varepsilon_0 \sigma T_s^4$ where L in this case is determined by the blackbody temperature. In the results given here, the emissivity of both the blackbody and the thermopile are assumed to be 1.0. A plot of these points is shown in Fig. 4. The slope of the line connecting these points gives $\frac{1}{\eta} = 178\ Wm^{-2}mv^{-1}$ for this particular instrument.

The k value in Eq. (3) may then be determined by plotting $(T_d^4 - T_s^4)$ as a function of $L - \varepsilon_0 \sigma T_s^4 - \frac{E}{\eta}$ assuming the sensitivity determined in the procedure described above. Plots for three of the calibration runs are shown in Fig. 5. The average value of k determined from these plots is k = 4.08.

As an additional check on the sensitivity determined by this particular calibration, measurements were made at 1716 LST, 4 November, 1975, in Fort Collins, Colorado with this instrument (battery circuit was not

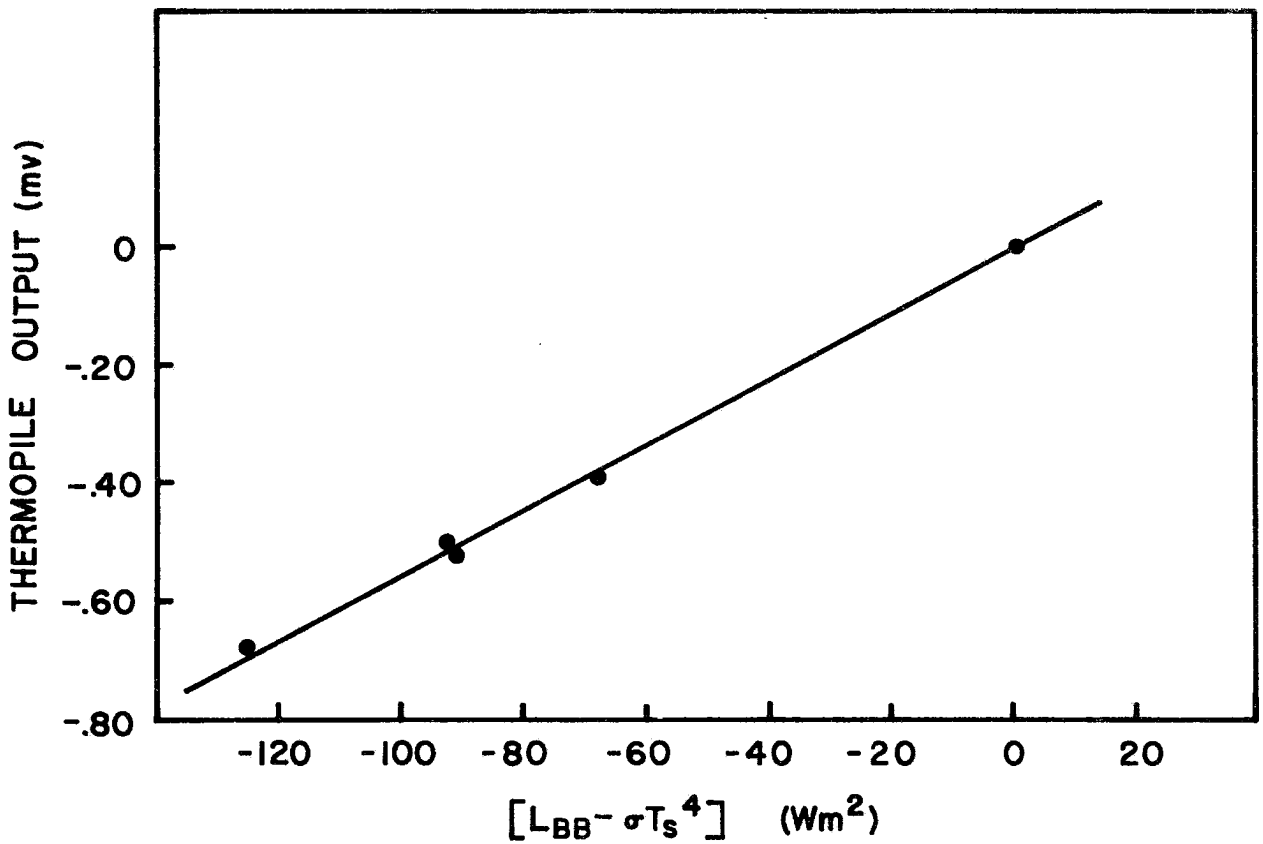

Figure 4. Thermopile output as a function of the difference in the radiative energy per unit area emitted by the blackbody and the thermopile surface.

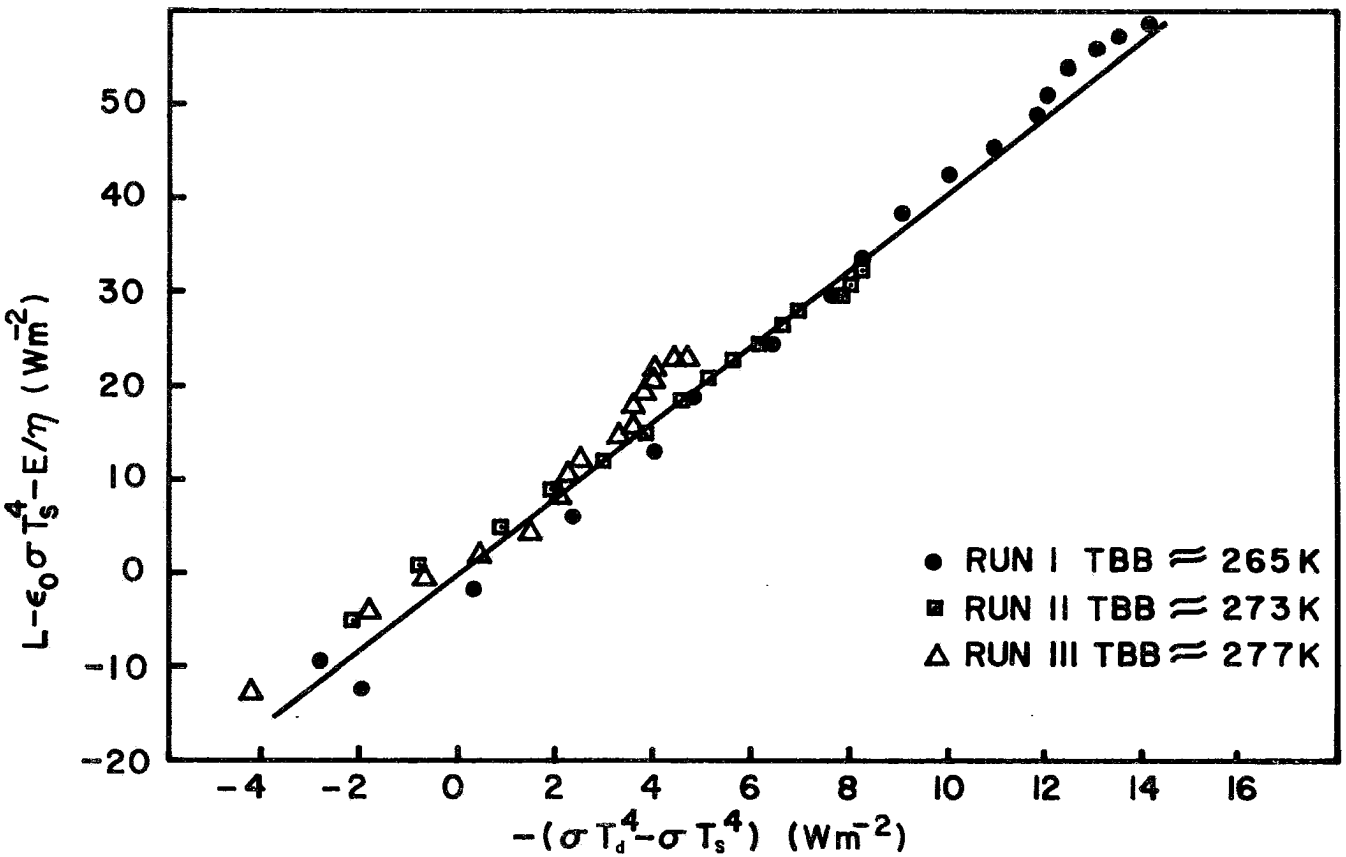

Figure 5. $L-\epsilon_0\sigma T_s^4-E/\eta$ as a function of $(\sigma T_d^4-\sigma T_s^4)$. The coefficient k is given by the slope of these points. T_{BB} is the approximate blackbody temperature at each calibration point.

used). The sky was virtually cloud free during the time of the measurements. Using the constants determined above the downward irradiance determined from the pyrgeometer output was 264 Wm^{-2}.

At the same time an infrared bolometer (2° field of view) with a spectral bandpass of 1.8 to 25 μm was used to independently measure the infrared radiance at a few zenith angles. Measurements were made after sunset, thereby eliminating any possible solar contamination. These radiance data are shown in Fig. 6. An integration over 2π steradians neglecting any azimuthal variation yields a downward irradiance value of 247 Wm^{-2}.

In addition to the data noted above, the 00Z radiosonde data from Denver, Colorado were used in a computation of $LW\downarrow$ at the surface. The computation technique described by Cox (1973) yielded a $LW\downarrow$ value of 263 Wm^{-2}.

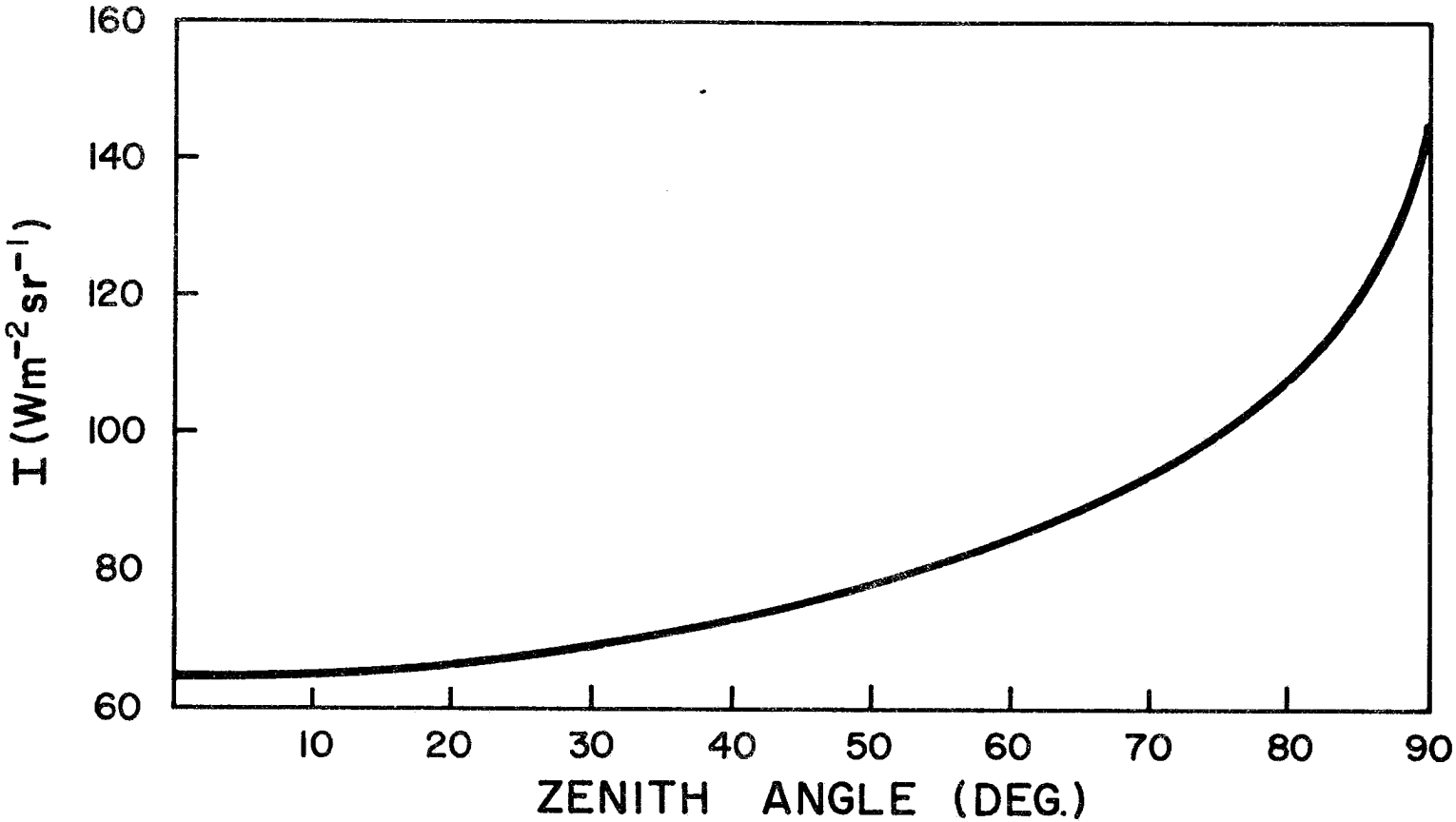

Figure 6. Radiance as a function of zenith angle in the spectral bandpass of 1.8-26 μm at 1716 LST, 4 November 1975, Fort Collins, Colorado.

IV. Temperature Corrections for Pyrgeometer Measurements

Ideally, the errors enumerated in section II may be eliminated by accurately measuring the dome and sink temperatures. The temperature of the sink may be used to calculate the $\varepsilon_o \sigma T_s^4$ term in Eq. (1) and eliminate (to within the accuracy of the temperature measurements) the δL_T and δL_B terms in Eq. (2). The δL_{DS} term may then be evaluated as $k\sigma(T_d^4 - T_s^4)$ in the data reduction. This method of reducing the data requires that the thermopile output be determined in order to calculate the $E(c_1 + c_2 T_s^3)$ term in Eq. (1). Consequently, to make pyrgeometer measurements by directly applying Eq. (1), three parameters; T_d, T_s, and E must be determined in order to calculate each irradiance value. Furthermore, the temperatures should be resolved absolutely to an accuracy of $\sim$.1 C. This accuracy may be difficult to obtain for the dome temperature since, in some situations this temperature may not be constant over the entire dome. The thermopile output may also be difficult to measure accurately since it may range from approximately .5 to -.5 mv and should typically be resolved to approximately 10 μv.

Although the direct calculation of the irradiance from Eq. (1) may provide the greatest accuracy, there may be applications when less accurate measurements are acceptable or it is not feasible to make direct measurements of T_d, T_s, and E. For example, in some situations, air temperature (or total air temperature on an aircraft) may be sufficient to specify the δL_T and δL_B terms in Eq. (2).

In this section the possible errors identified in section II and corrections for these errors are considered in detail. The magnitude of these errors is evaluated for aircraft data collected during a radiation flight made during GATE. The results presented in this section may also

be useful in evaluating whether or not data reduction based upon the three variables T_d, T_s, and E is warranted for a specific application.

A. Battery Voltage Uncertainty

The voltage, E_A, shown in Fig. 2, is supplied by a small mercury cell mounted inside the instrument. Although the voltage output of the mercury cells used is generally quite stable, it may vary slightly with age and temperature. The contact resistance of the batteries may also cause some fluctuations in the actual voltage applied to the circuit. These small variations may result in large variations in the pyrgeometer output.

Referring to the left-hand side of Fig. (2) it is evident that

$$\delta L_B = \frac{(E_o - E_A)\, R_o}{(R_{T1} + R_2 + R_o)\eta} \qquad (4)$$

where E_o is some standard voltage, (E_o = 1.35 volts), $1/\eta$ is the instrument sensitivity, and

$$R_{T1} = \frac{R_1 R_T}{(R_1 + R_T)} \qquad (5)$$

Typical values of $\delta L_B/(E_o - E_A)$ calculated form Eq. (4) are shown in Fig. 7. It is apparent that the largest absolute errors due to the battery voltage uncertainty occur at warmer temperatures. The relationship shown in Fig. 7 indicates that a .10 volt variation in the battery voltage will result in a 33 Wm^{-2} variation in instrument output at 25°C. The variations become absolutely smaller at colder temperatures, although the relative variation may be as large.

During GATE, the pyrgeometer batteries were mounted in the cabin of the NCAR Saberliner aircraft to prevent battery failure at low

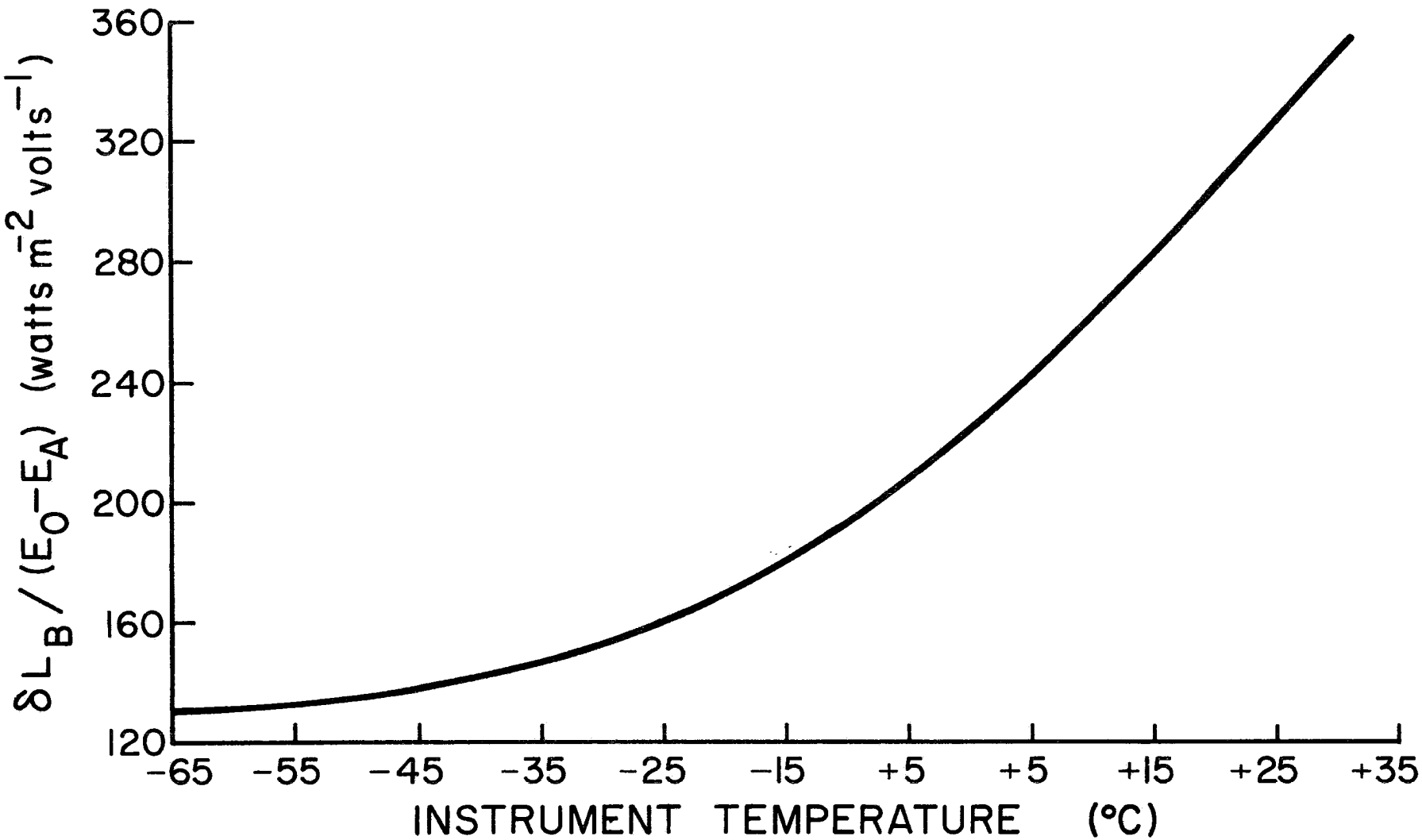

Figure 7. $\delta L_B/(E_o - E_A)$ as a function of temperature.

temperatures. The voltages of the mercury cells varied from 1.50 to 1.35 volts during the experiment. Although the cells used for these pyrgeometers did not appear to be as stable as those typically used in the instrument, these variations, unless properly accounted for, would result in an error of 45 Wm^{-2} at 25°C.

B. Non-Linearity of Pyrgeometer Performance with Temperature

To determine the errors introduced by the non-linearity of the battery circuit, the term $\varepsilon_0 \sigma T_s^4$ in Eq. (1) is compared to the corresponding output of the instrument. Using Eq. (4), this error may be written as

$$\delta L_T = \varepsilon_0 \sigma T_s^4 - (E_0 R_0) / (R_{T1} + R_2 + R_0)_n \qquad (6)$$

The emissivity, ε_0, of the thermopile surface is approximately 1.0. To determine a more exact value for ε_0, it was assumed that $\delta L_T = 0$ at 15°C, the temperature at which sensor sensitivities were determined by Eppley.

Values of δL_T calculated using Eq. (6) are shown in Fig. 8 as a function of cold junction temperature. For temperatures between 30°C and -25°C, the value of δL_T is less than ± 8 Wm^{-2}. However, at temperatures less than -25°C, the value of $|\delta L_T|$ increases rapidly with decreasing temperature.

The δL_T errors at low temperatures are not only large in the absolute sense, but may be extremely large in the relative sense. Consider, for example, a hypothetical case in which the actual downward longwave irradiance is 70 Wm^{-2} at an altitude where the air temperature is -55°C and 80 Wm^{-2} at an altitude where the temperature is -45°C. If pyrgeometer measurements were made at these levels the actual instrument output would be 125 Wm^{-2} at -55°C and 117 Wm^{-2} at -45°C provided the thermopile

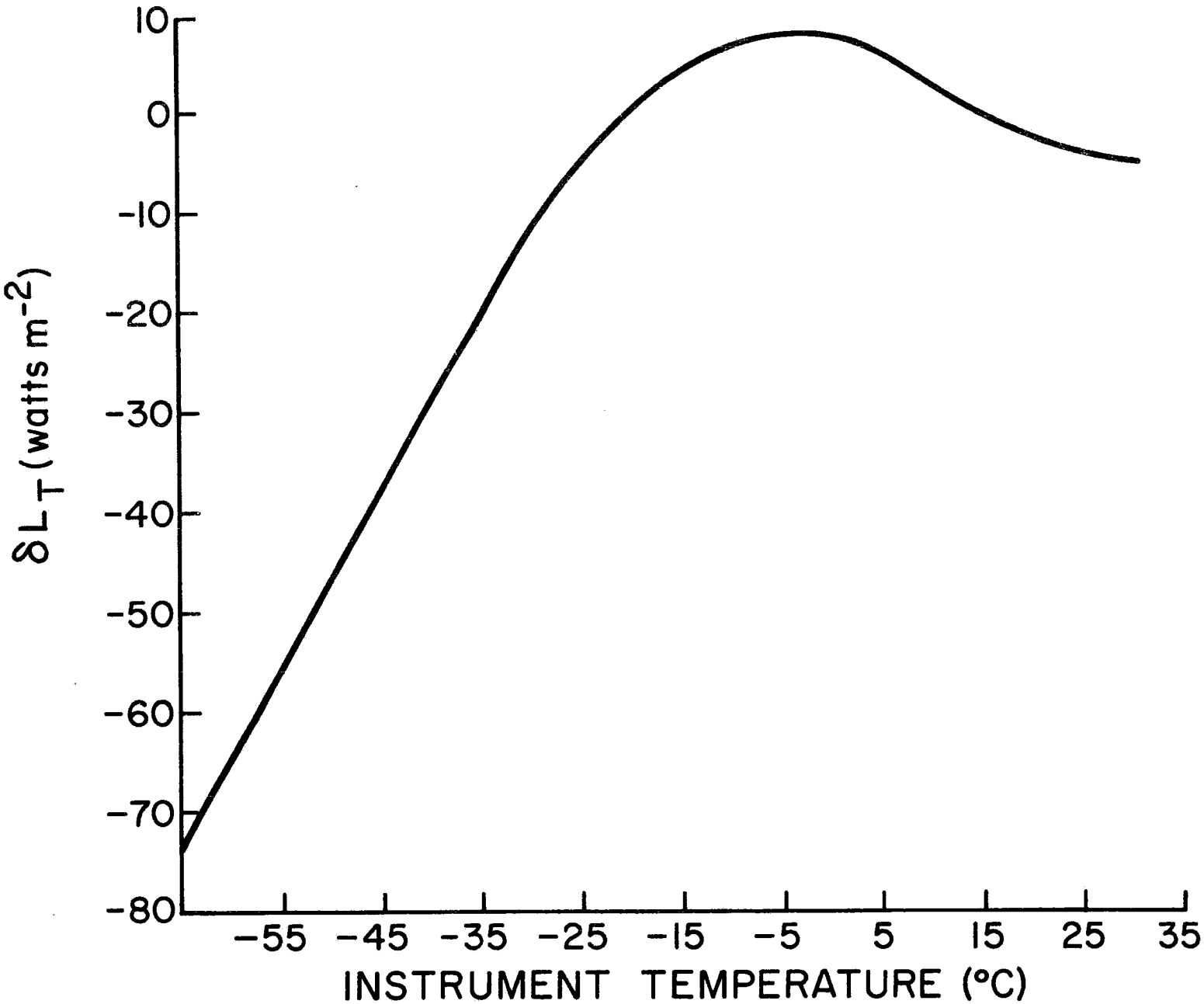

Figure 8 . δL_T as a function of temperature.

output is accurate. Not only are these values in error by more than 40 Wm^{-2}, the irradiance indicated by the sensor would actually increase with height. This apparent increase of irradiance with height has been observed on some aircraft data. It is important to note, however, that if both the upward and downward facing sensors are at the same temperature, the δL_T correction may not significantly affect the net irradiance at a level.

C. Dome-Sink Temperature Differences

To determine the magnitude of the term $k\sigma(T_d^4 - T_s^4)$ it is necessary to make measurements of T_d and T_s or $T_d - T_s$ and the mean temperature. It is not obvious, however, how the temperature of the dome T_d should be determined, since the temperature may not be constant over the entire dome. In some cases, a single point measurement may be representative of the average dome temperature. In cases where solar heating of the dome is a problem, a correction based on a point measurement of T_d may not be sufficient since the temperature at that point may depend on the geometry of the instrument and the direct solar radiation.

The instruments used on the Sabreliner had a small bead thermistor attached to the inside of the KRS-5 hemisphere. In some instances the temperature determined at this single point may be significantly different than the average dome temperature. However, if variations in this temperature are representative of the average temperature variations of the dome, the $k\sigma(T_d^4 - T_s^4)$ relationship may be maintained with the proper choice of k. This k, however, may differ from the laboratory value of k.

An attempt was made to determine the constant k from a data set collected during GATE. The particular data used were collected during a NCAR Sabreliner flight made on August 17, 1974, approximately 320 km

off the coast of Senegal, West Africa. During this flight, a uniform stratocumulus deck with a top at approximately .9 km was observed. Haze to 4.73 km and some high cirrus were also reported. The flight consisted of 19 constant pressure-altitude legs, each of a duration of approximately four minutes. The legs were flown at altitudes ranging from 9.45 km to 15 m above the sea surface.

The NCAR Sabreliner was equipped with both upward and downward facing pyrgeometers during GATE. The millivolt outputs from these instruments were amplified by a 0-5 volt range and were recorded on magnetic tape. Dome and sink temperatures were determined using thermistors mounted within the instrument and were also recorded on magnetic tape.

To determine k at a particular level, it is assumed that the infrared target viewed by the instrument is constant during that leg. The output of the instrument (corrected for δL_B and δL_T errors) is then correlated linearly with $\sigma(T_d^4 - T_s^4)$. The slope of the linear relationship between the instrument output determines k, as shown, for example, in Fig. 9.

The results shown in Fig. 9 were determined at a constant pressure level of 453 mb using the upward facing sensor. The temperature at this level was -10.4°C and was preceded by a descent from a level of 288 mb and -33°C. Consequently, since the sink temperature responds slowly to this temperature change, T_d is greater than T_s during the entire leg although the difference between T_d and T_s decreases with time. The linear fit at this level is excellent with k having a value of 3.67. The values shown in Fig. 9 represent 3 second averages. At all levels and for both instruments, a similar analysis was performed using values

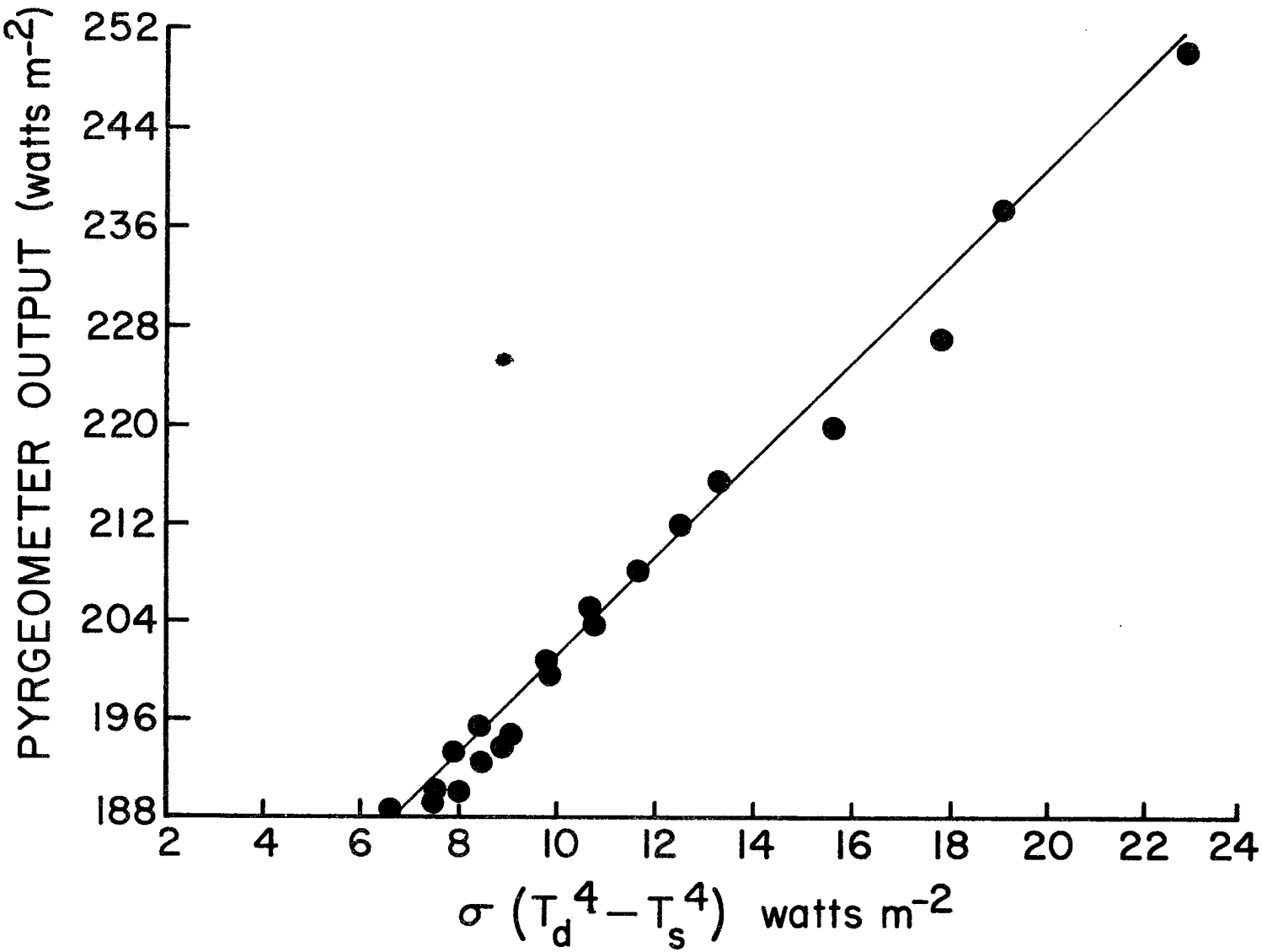

Figure 9. Pyrgeometer output as a function of $\sigma(T_d^4 - T_s^4)$. Each point represents a 3 sec average although only points every 15 secs are given here for clarity.

averaged over three second intervals.

Values of k determined at other levels are shown in Fig. 10. In a few cases the k values shown in Fig. 10 were determined subjectively. This was done when instrument output variations were obviously due to variations in the infrared target. In other cases, no clear linear trend was discernable and k values could not be determined. This was particularly true for flight levels made in the vicinity of the stratus or when $T_d \simeq T_s$ during the entire leg.

The values of k for the downward facing sensor have an average value of 1.20. The value at -33°C, however, is significantly larger than 1.20, although it should be noted that the variation of $T_d - T_s$ was small in this case. The values of k for the upward facing sensor vary between 1.0 - 1.8 for temperatures warmer than 0°C. However, at temperatures colder than 0°C, the k values increase with decreasing temperatures. This variation of k may, however, be due in part to the variation of the angle of attack of the aircraft as it flies at different altitudes. In the future, additional data may be analyzed to determine k values at cold temperatures and different angles of attack. Several flights were made under cloud free conditions during GATE which should eventually prove to be useful in establishing the validity of making corrections with a single point measurement of the dome temperature.

D. Application of Corrections to Aircraft Data

The temperature corrections described above were applied to a data set collected during GATE. The flight considered was flown on August 17, 1974, and is the same flight from which data were used previously to determine the value of k in the δL_{DS} correction term. The pyrgeometer

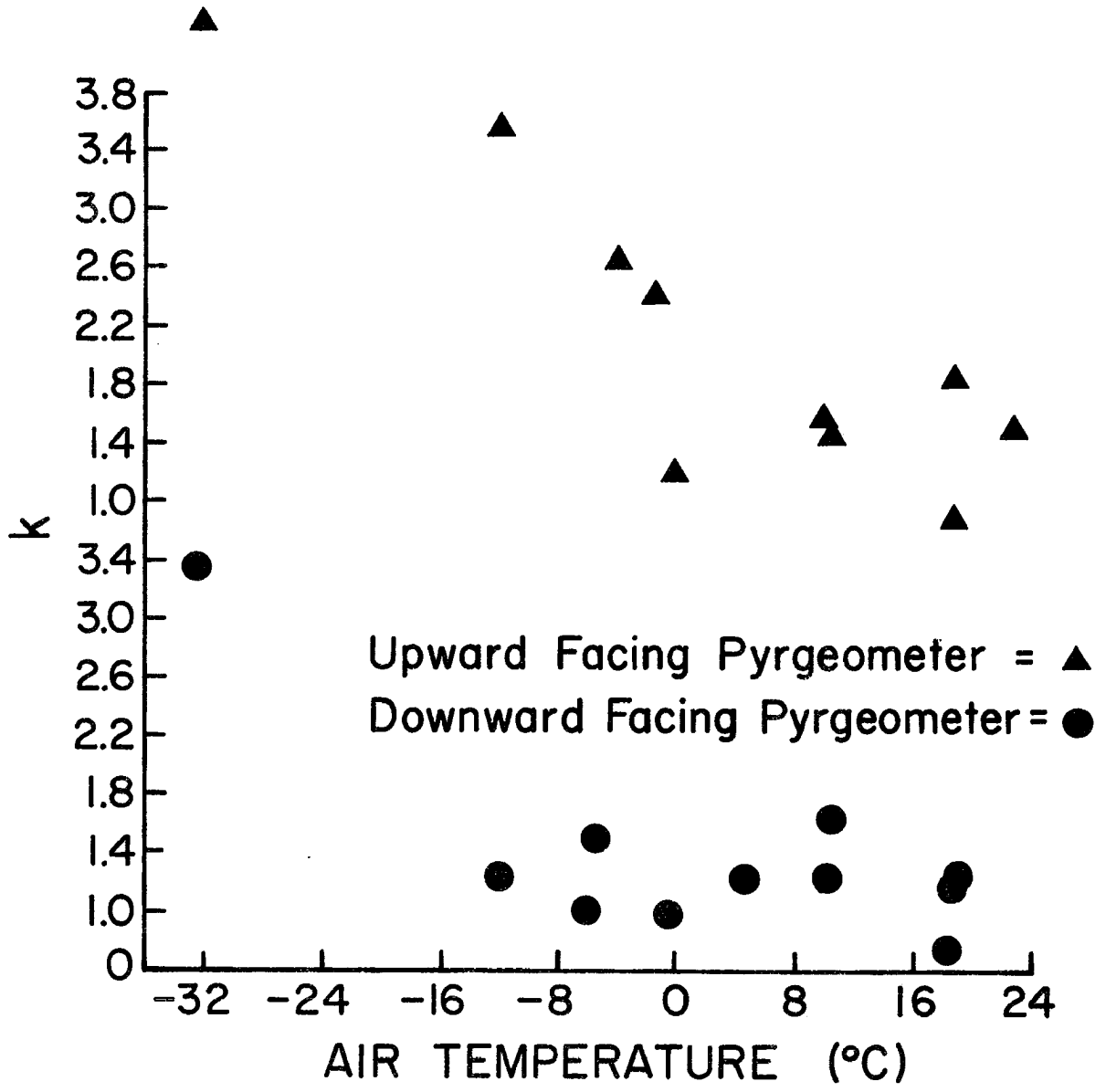

Figure 10. k values as a function of temperature for downward and upward facing pyrgeometers.

battery voltages needed to make the δL_B corrections were 1.49 volts for both the upward and downward facing sensor. The corrections were performed using three second averages of uncorrected pyrgeometer outputs and thermistor measurements. The k needed to make the δL_{DS} correction was assumed to 1.35 for both instruments at all levels.

The downward irradiance (measured by the upward facing pyrgeometer) averaged over the last two minutes of each leg is shown in Fig. 11 for both the corrected and uncorrected data. The average leg was approximately four minutes long. As indicated in Fig. 11, the corrected and uncorrected values differ by as much as 80 Wm^{-2} at 1000 mb. These differences decrease to approximately 30 Wm^{-2} at 300mb.

The flight made on August 17 actually consists of two separate profiles, each made in a descending mode. The agreement shown in Fig. 11 between the measurements made during each profile is excellent considering that the second profile was made approximately 100 km from the first.

The magnitudes of the individual correction terms averaged over the last two minutes of each leg are shown as a function of pressure in Fig. 12 for Run I. The δL_B term accounts for a large portion of the correction since battery voltages were relatively large on this flight. The large differences at low levels are almost totally due to this high voltage. The correction δL_{DS} resulting from temperature differences between the dome and sink differences has an average value of 10-12 Wm^{-2}. This results from the dome having a slightly warmer steady state temperature than the sink of the instrument. The correction for the nonlinearity of the pyrgeometer circuit averages ± 4 Wm^{-2}. Although this is a relatively small correction, it may be, as shown by Figure 8, much greater for flights made at very cold temperatures.

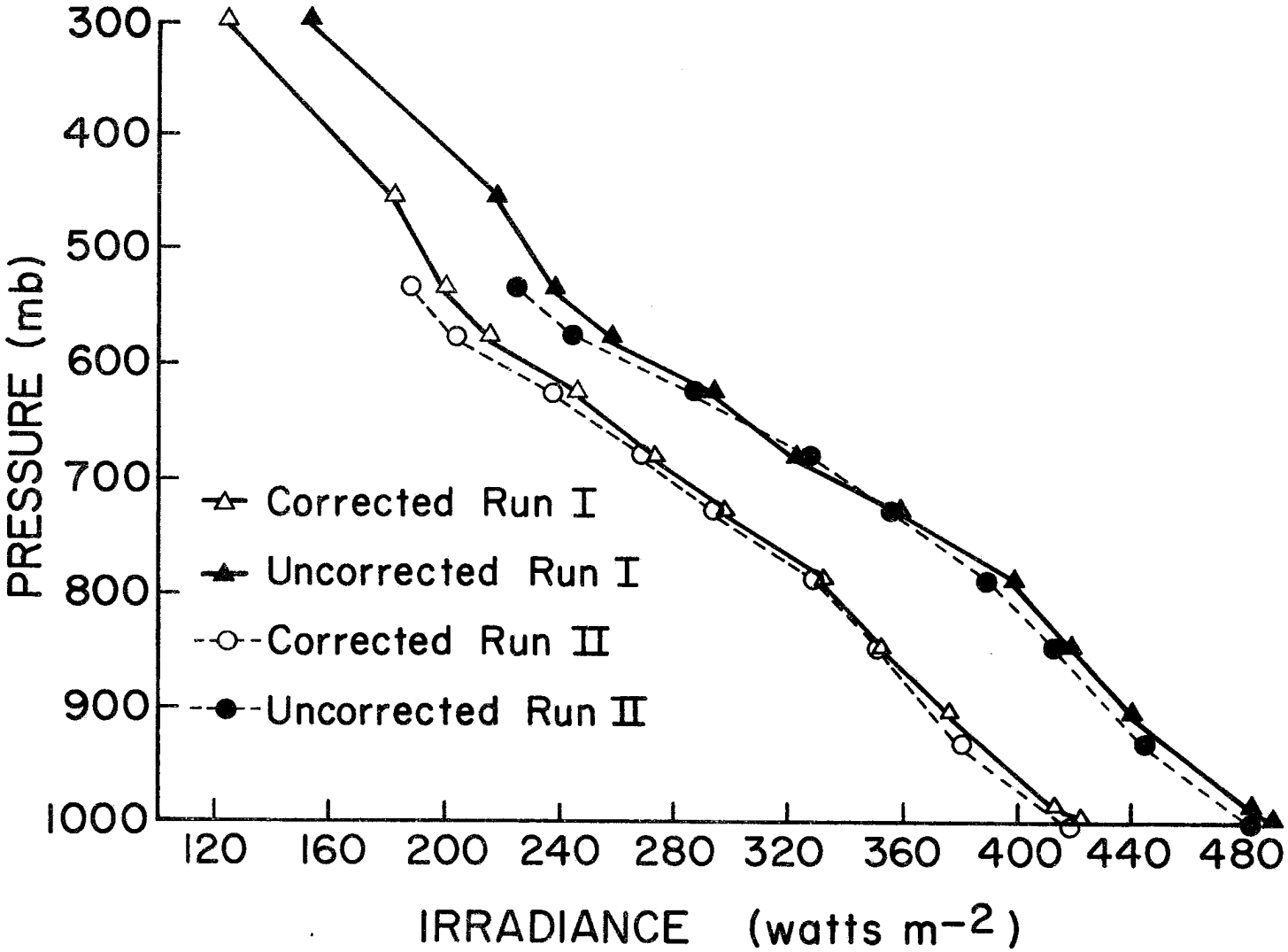

Figure 11. Comparison of corrected and uncorrected pyrgeometer measurements of L↓ for August 17, 1974, Sabreliner flight. Average for the last two minutes of each leg.

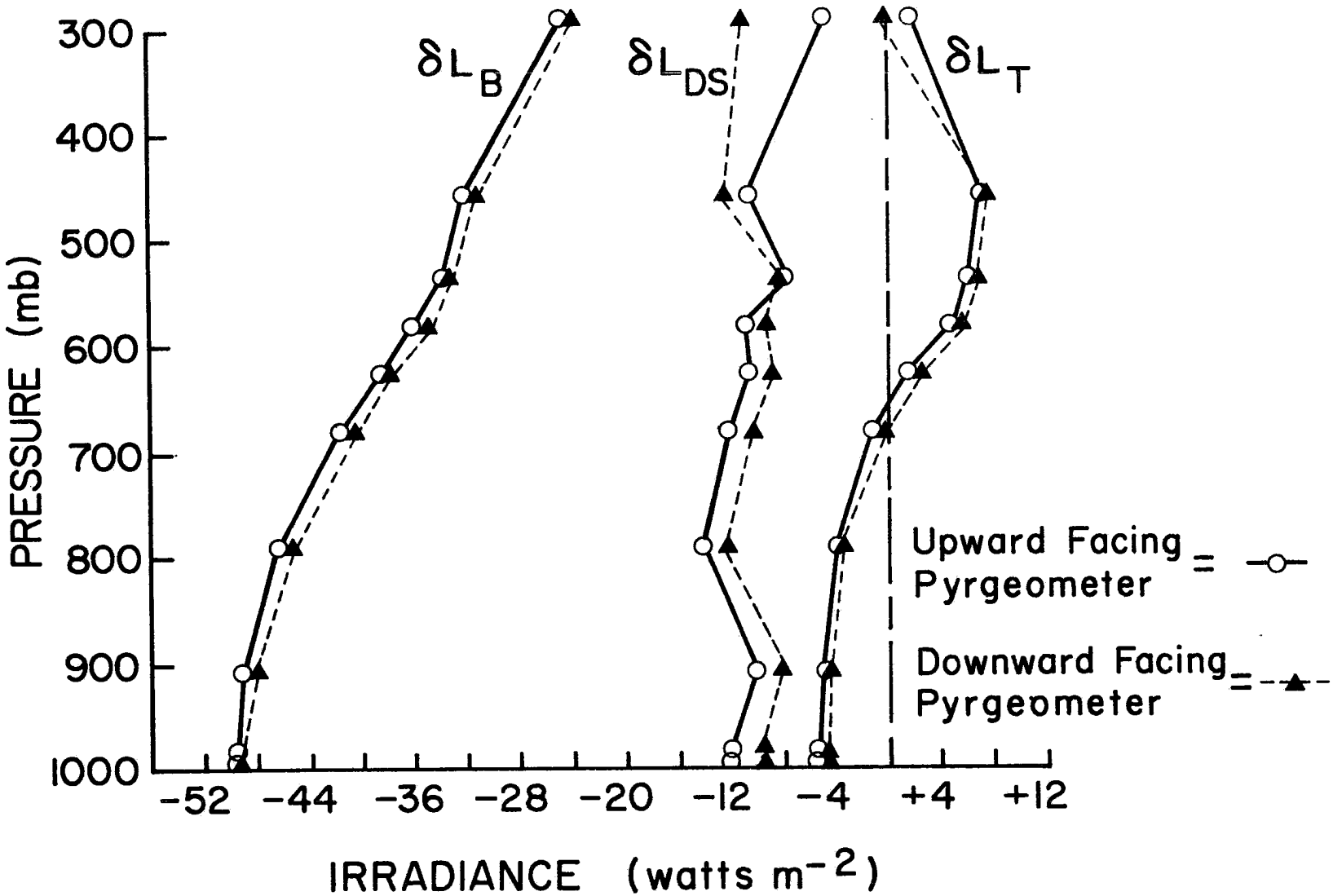

Figure 12. Correction terms as a function of altitude for August 17, 1974, Sabreliner flight.

The correction terms for the downward facing pyrgeometer are also shown in Fig. 12. These corrections are nearly identical to the corrections for the upward facing instrument. Consequently, the infrared heating rate calculated from the corrected and uncorrected data should not be significantly different. Heating rates calculated with corrected and uncorrected data for the highest layers of these profiles differ by .4°C day $^{-1}$. In the lowest layers the difference is less than .1°C day. The larger differences in the top layers are principally due to the divergence of the δL_{DS} correction terms shown in Fig. 12. If a larger value of k had been used in correcting the upward facing pyrgeometer at the upper two levels, the differences in the heating rates would have been smaller.

As shown in A74, the dome sink correction term may be useful in minimizing the errors which occur before dome and sink temperatures stabilize following ascents and descents. If the irradiance field at a level is assumed to be constant during the entire leg, the difference between measurements made during the beginning and end of a leg should be zero if there is no instrument temperature lag. The difference between the average of the downward irradiance for the first two minutes and the average for the last two minutes was calculated for the 19 constant pressure altitudes flown on the August 17 flight. The differences are tabulated in Table I for the uncorrected and corrected data. The differences are 3-4 Wm^{-2} smaller for the corrected data than the same difference calculated with the uncorrected data. The differences are large for both the corrected and uncorrected at the three highest levels. These differences occur at the levels where k was determined to be larger than the 1.35 value used to make these corrections.

Table I. Average of first two minutes minus average of last two minutes of each leg for upward facing pyrgeometer.

RUN I			RUN II		
P(mb)	Uncorrected (Wm^{-2})	Corrected (Wm^{-2})	P(mb)	Uncorrected (Wm^{-2})	Corrected (Wm^{-2})
288	-26.1	-21.1	532	-15.2	-12.3
453	30.1	21.3	576	5.3	2.8
533	8.7	4.8	655	1.4	0
578	4.3	.1	675	5.8	1.9
626	9.8	3.9	730	2.4	0
679	7.5	2.4	786	4.0	-2.3
790	3.8	0	847	2.5	-1.3
908	6.4	1.3	927	1.5	.9
988	4.7	2.1	1011	6.8	3.3
1000	.4	1.9			
Average (excluding 283 and 453 mb levels)	5.7	2.1	Average (excluding 532 mb level)	3.7	.7

A further comparison of corrected and uncorrected data is shown in Figs. 13a and b for the upward facing sensor. These measurements were made from the Sabreliner on July 30, 1974. The corrections for dome-sink temperature differences were made with a value k of 1.35. The flight pattern flown during the 15 minutes of data shown consisted of a descent from 870 mb to 942 mb from 13:45:00 GMT to 13:48:30 GMT. The 942 mb pressure level was maintained until 13:50:30 GMT at which time the aircraft ascended to 925 mb and maintained this level until 13:56:00 GMT. The data shown from 13:57:30 GMT to 13:60:00 GMT were recorded at a pressure level of 910 mb. The transient response of the instrument is quite evident in the uncorrected data, with variations as large as ± 4 Wm^{-2} occurring during a particular leg. In most cases, the corrections reduce these variations to less than ± 1.5 Wm^{-2}. The absolute values of the corrected data are decreased by ~20 Wm^{-2}.

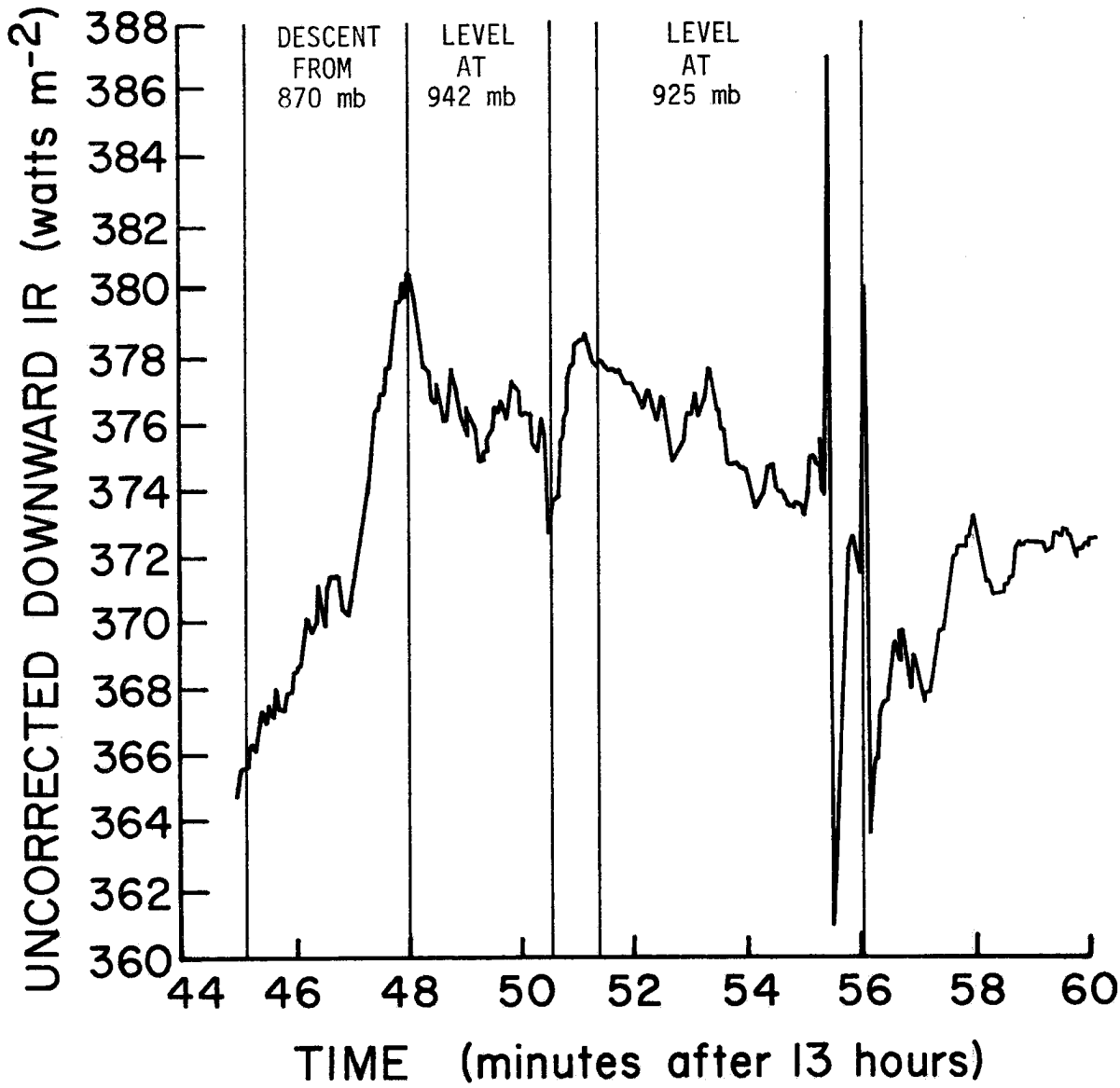

Figure 13a. Uncorrected pyrgeometer measurements for July 30, 1974, Sabreliner flight. Time is given in minutes after 1300 GMT.

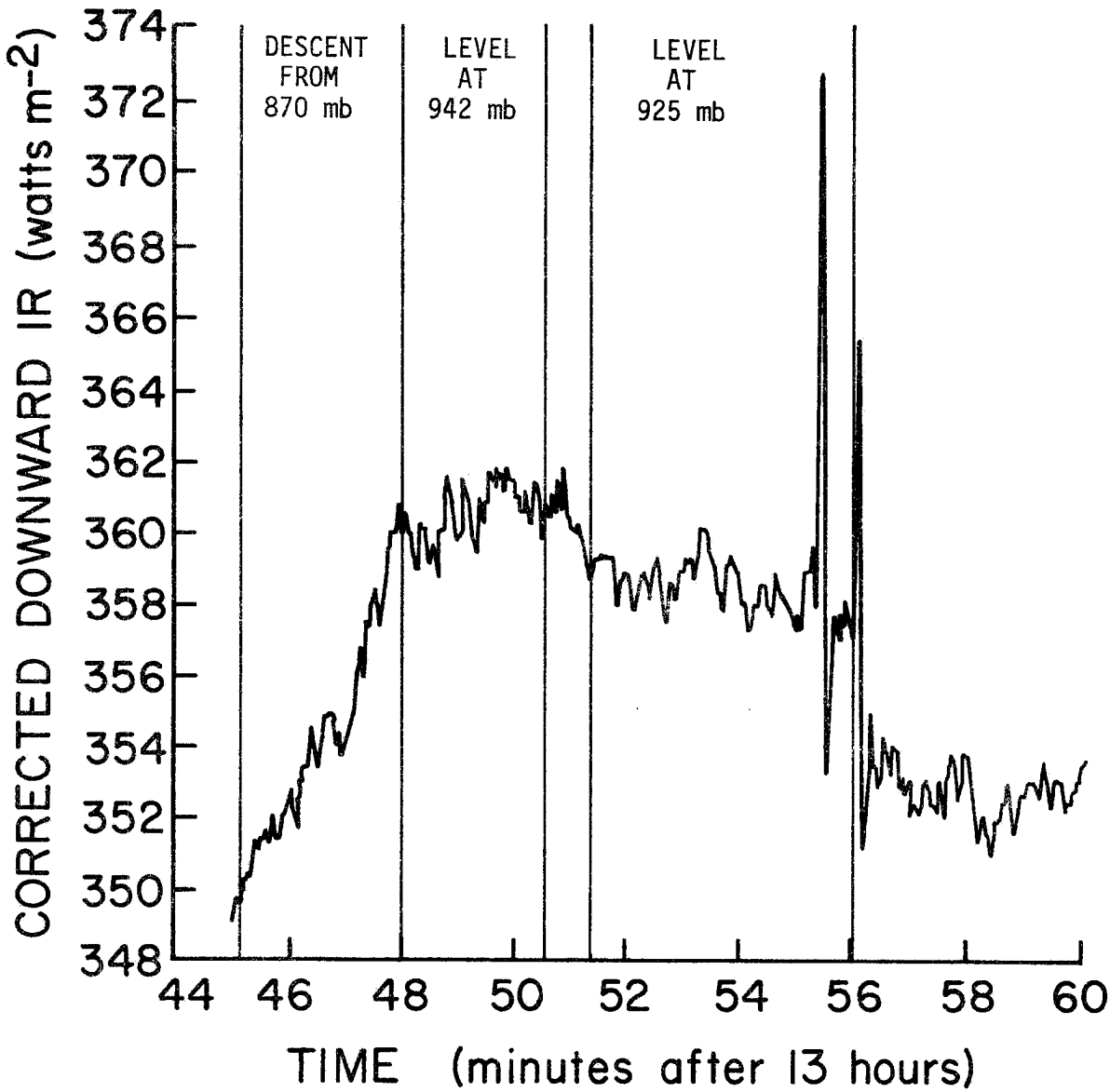

Figure 13b. Corrected pyrgeometer measurements for July 30, 1974, Sabreliner flight. Time is given in minutes after 1300 GMT.

V. Empirical Corrections for Direct Solar Heating of Pyrgeometer

As mentioned above, the airflow over pyrgeometers mounted on aircraft tends to minimize the heating of the KRS-5 hemisphere due to the absorption of solar radiation. However, for slower moving aircraft (e.g. the U.S. DC-6 during GATE) the airflow may be insufficient to prevent solar heating of the dome. This is evident in the $L\downarrow$ and $H\downarrow$ measurements shown in Fig. 14. These measurements were made at 1300Z, September 7, 1974, over the GATE array from the NOAA RFF DC-6. The pressure flight level of the aircraft during this period is 1002 mb and the free air temperature is approximately 25.5°C. The $L\downarrow$ data shown in Fig. 14 appears to be strongly correlated to the downward solar irradiance. Physically, however, one would expect very little or slightly negative correlation between these two parameters at this level in the atmosphere.

The positive correlation between the downward longwave and downward shortwave is consistent with the variations in temperature differences between the dome and sink. This is shown in Fig. 15 where 30 second averages of a correction factor based on measured dome and sink temperature differences are shown to be correlated with the downward irradiance values averaged for the same time interval. It should be noted that the intercept of the temperature correction shown in Fig. 15 has not been calibrated absolutely; the relative variations, however, should be consistent.

The data presented in Figs. 14 and 15 indicate that a correction on $L\downarrow$ for the solar heating may be expressed directly in terms of the downward SW irradiance. This method of correcting the heating of the dome due to solar radiation on slower moving aircraft is appealing since the

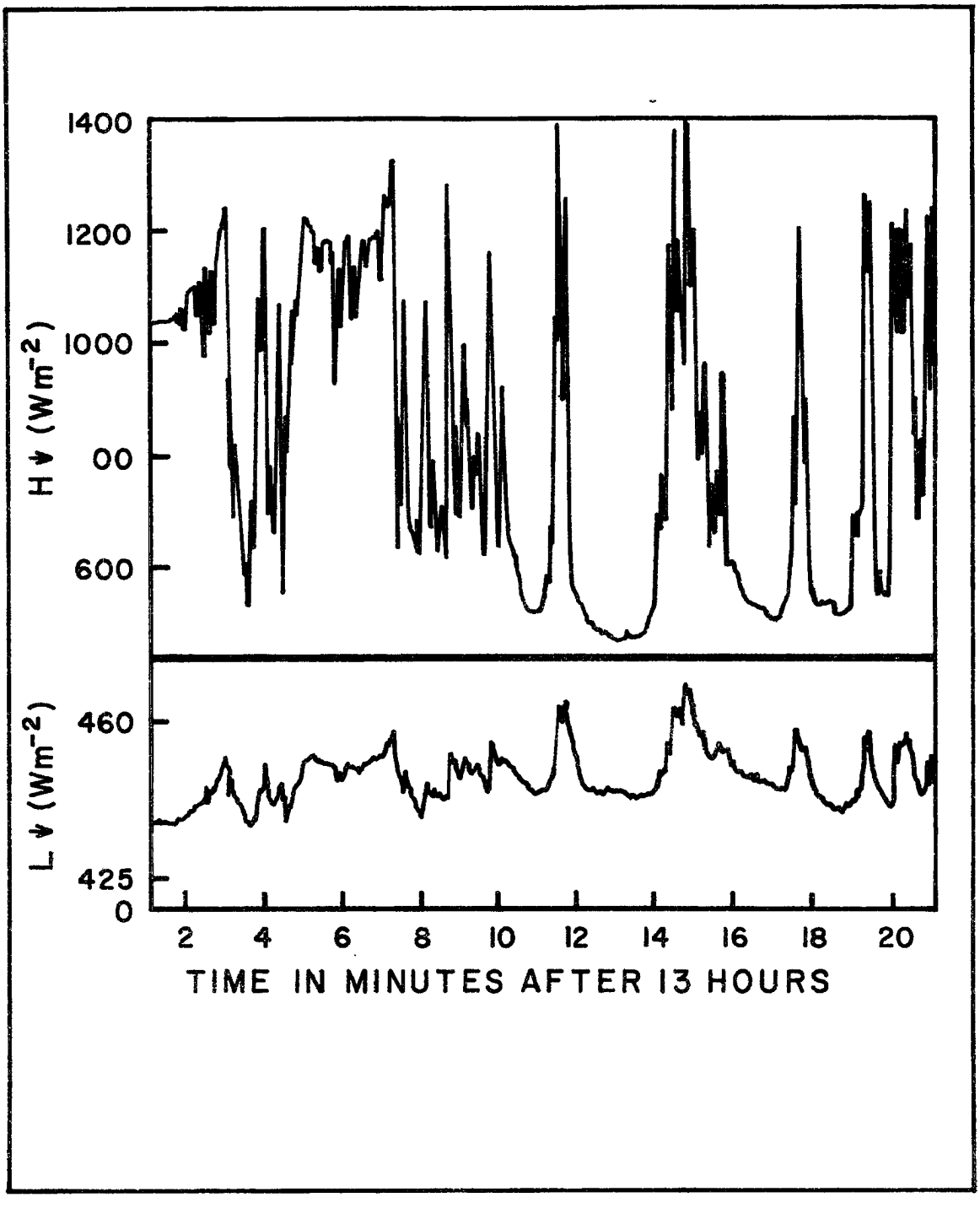

Figure 14. [illegible] and $H_{\downarrow}$ measurements. September 7, 1974, 1301-1321 GMT.

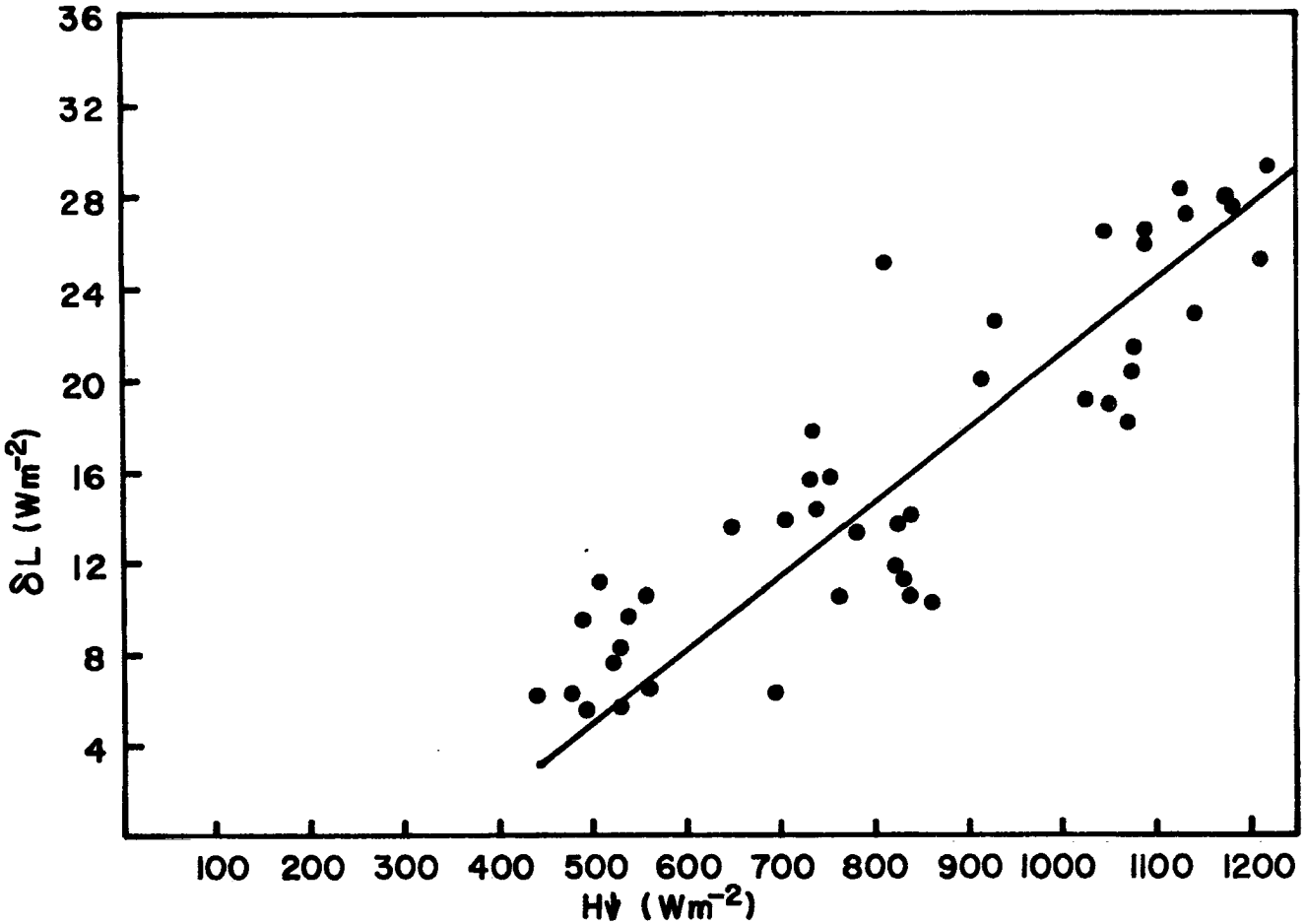

Figure 15. L↓ correction based on difference between dome and sink temperature as a function of H↓. All values are 30 second averages.

dome temperature determined at a single point may not give a representative value of the average dome temperature at various solar geometries.

To determine a correction formula based on the incident solar radiation, an equation of the form

$$\delta L = a\, H\downarrow + b \left.\frac{\partial H\downarrow}{\partial t}\right)_{-} \qquad (7)$$

is assumed where $H\downarrow$ is the incident downward shortwave irradiance and a and b are constants. The derivative of the downward shortwave irradiance represents a backward derivative in time and is included in Eq. (7) to represent the "past" heating history of the dome.

Some care must be used in determining the constants a and b in Eq. (7) since the corrections are on the order of 5% of the absolute value of $L\downarrow$. Ideally, to determine these constants from data it is desirable to have measurements in a region where the downward irradiance is constant and the downward shortwave varies with time. In the tropical atmosphere such conditions are approximately satisfied near the surface with a scattered cloud field above. This property is illustrated by noting the downward irradiance fields calculated for a typical clear sky tropical atmosphere shown in Fig. 16. Note that if a black cloud ($\varepsilon = 1.0$) with a cloud base at 950 mb was placed in this atmosphere, the downward irradiance near the surface would only differ slightly from the clear sky value. Note, further, that if measurements are made beneath a broken homogeneous cumulus field the downward irradiance would remain fairly constant since the pyrgeometer is a hemispheric instrument. The downward shortwave irradiance in this case, however, would vary significantly due to the modulation of the direct radiation by the clouds.

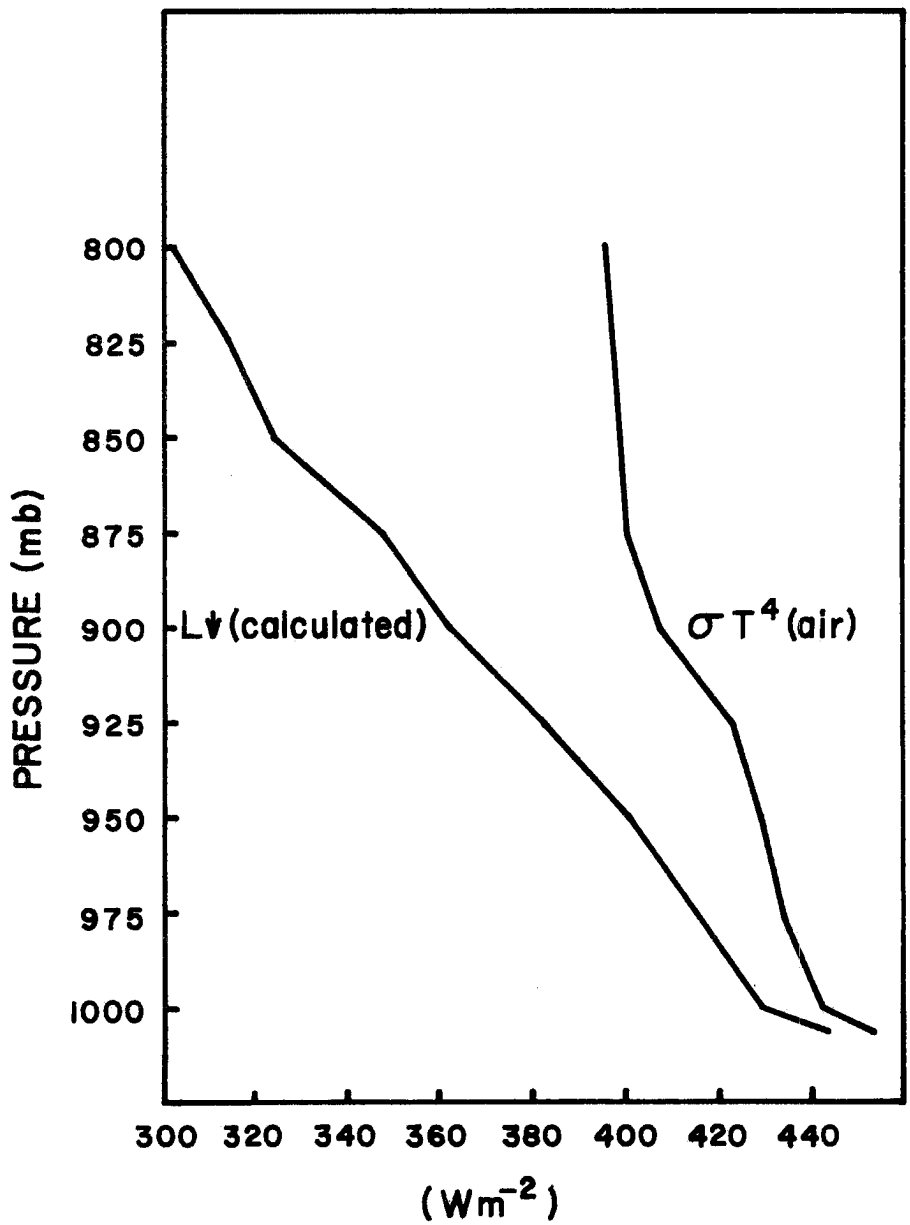

Figure 16. Calculated downward I.W irradiance for a typical tropical atmosphere and σT^4(air) for this same atmosphere.

The actual downward longwave is assumed to be constant during the 1301-1308 time period of the data shown in Fig. 14 in order to determine a and b in Eq. (7). The coefficient a is determined by plotting the measured L↓ as a function of H↓ at points where $\frac{\partial H\downarrow}{\partial t})_-$ [1] is approximately zero ($\leq$ 15 $Wm^{-2}sec^{-1}$). L↓ data collected from 1301 to 1308 GMT (see Fig. 14) and meeting these criteria are plotted in Fig. 17 as a function of H↓. Although there is some scatter of these points, the fit is not unreasonable considering that the actual L↓ may vary by a few Wm^{-2}. This slope also compares reasonably with the slope determined from dome and sink temperature differences (Fig. 17). The coefficient, a, may also be determined by noting that if Eq. (7) is averaged over some interval $t_1 < t < t_2$ the expression that results is

$$\overline{\delta L} = \overline{aH\downarrow} + \frac{b[H\downarrow(t_2) - H\downarrow(t_1)]}{t_2 - t_1} \qquad (8)$$

Note that if the interval is sufficiently large, the second term may be neglected reducing Eq. (8) to

$$\delta\overline{L} = a\overline{H\downarrow}. \qquad (9)$$

Fifteen second averages of L↓ and H↓ are plotted in Fig. 18 for the 1301-1322 time period. The data have been subjectively stratified into three time periods to account for the apparent large-scale variations in the actual L↓. Although there is a significant amount of scatter the variation of the measured L↓ with H↓ is similar to that shown in Fig. 17.

---

[1] $\frac{\partial H\downarrow}{\partial t})_-$ is defined here as $(H_i - H_{i-2}) / 2$ where H_i is the value of irradiance at the i^{th} second.

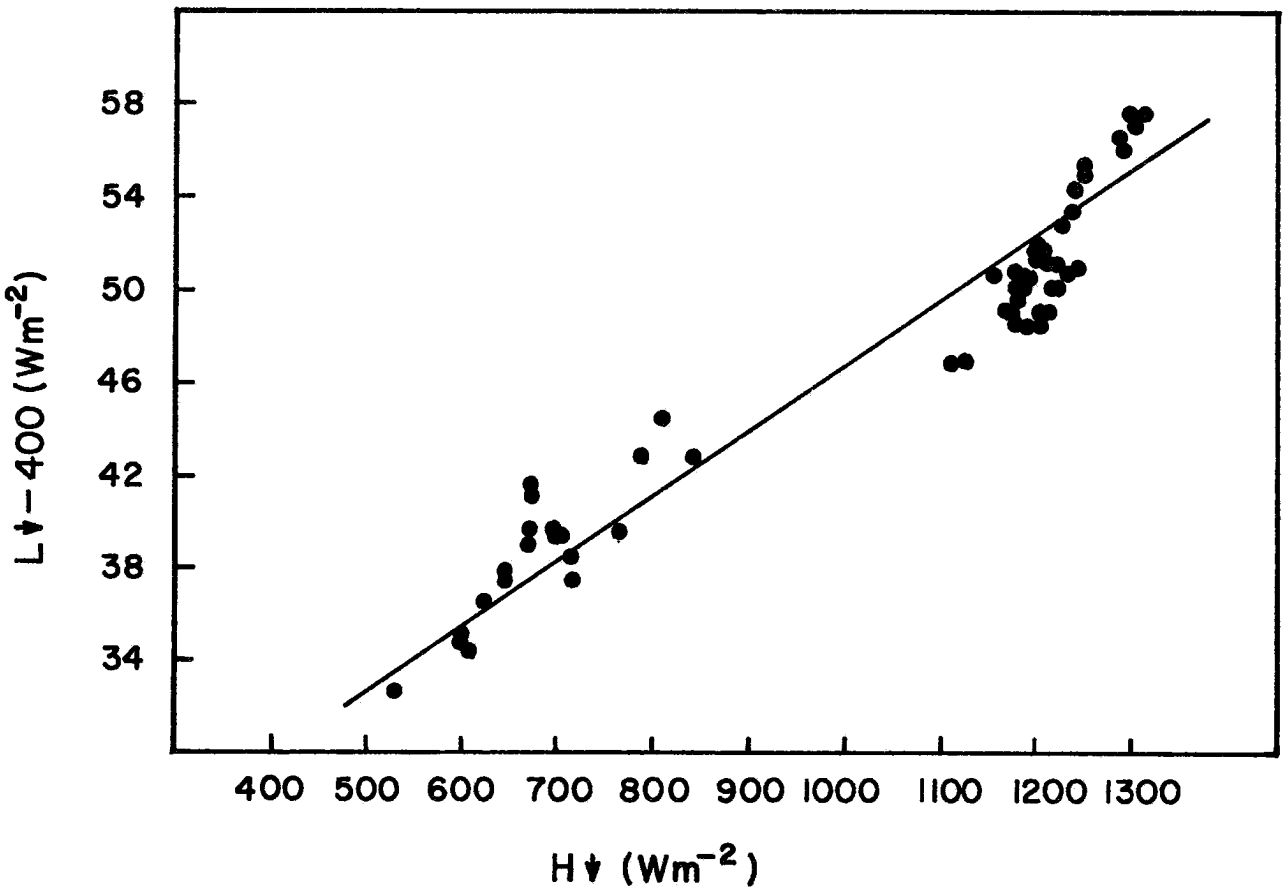

Figure 17. L↓ as a function of H↓ at points where $\frac{\partial \downarrow}{\partial t}) \leq 15$ Wm^{-2} sec^{-1}.

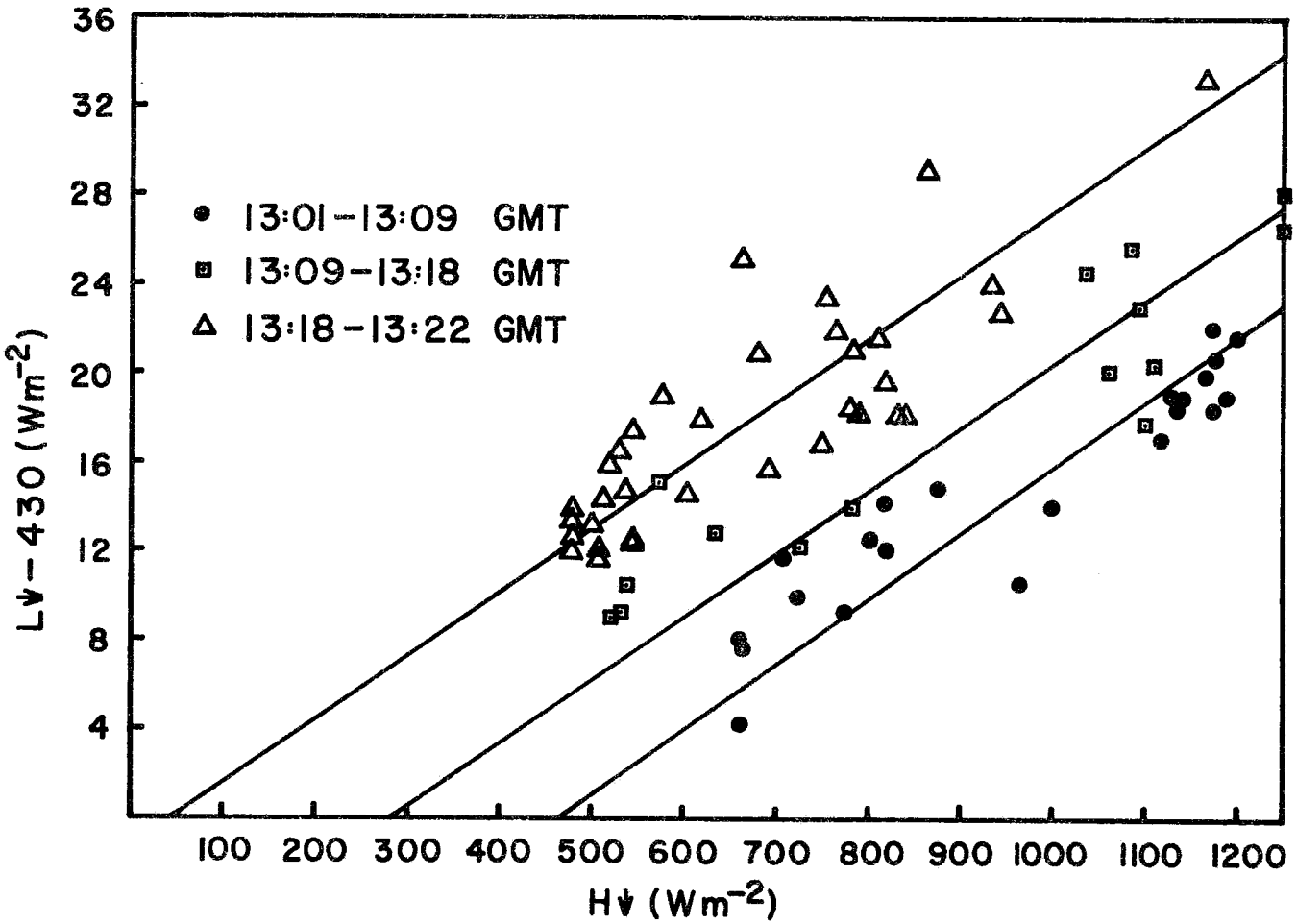

Figure 18. 15 second averages of L↓ and H↓ stratified into three separate time intervals.

The coefficient b in Eq. (7) may be determined by plotting $L\downarrow_{meas} - a\overline{H\downarrow} + \Delta L$ as a function of $\frac{\partial H\downarrow}{\partial t})_-$, where ΔL is a parameter which attempts to account for the value of the actual variations in the downward longwave. The factor ΔL was determined by assuming that the deviations of the points from the line shown in Fig. 17 may be attributed to real variations in $L\downarrow$. The deviations implied by this subjective analysis were plotted as a function of time and, subsequently, extrapolated to all data points.

A plot of $L\downarrow_{meas} - a\overline{H\downarrow} + \Delta L$ as a function of $\frac{\partial H\downarrow}{\partial t})_-$ was made for the 1301Z to 1322Z time period and is shown in Fig. 19. Although there is considerable scatter, the negative correlation is clearly discernable. Physically, this is consistent with the idea that $L\downarrow_{meas}$ will slightly lag the solar irradiance. The linear fit shown in Fig. 19 was determined subjectively.

The results presented above give an expression for the correction as

$$L\downarrow_{corr} = L\downarrow_{meas} - .0311\ H\downarrow + .0666\ \frac{\partial H\downarrow}{\partial t})_- \qquad (10)$$

This correction (which was determined from the 1301Z-1308Z data) was applied to the 1308Z to 1318Z time period of the September 7, 1974, DC-6 flight. The shortwave down, uncorrected and corrected longwave down for this period are shown in Fig. 20. The average value of $L\downarrow$ for this period is decreased from 449 Wm^{-2} for the uncorrected data to 427 Wm^{-2} for the corrected data. The standard deviation for this same period decreased from 7.0 Wm^{-2} to 3.9 Wm^{-2}. It is important to note that although the standard deviation is still relatively high, the variations in the corrected data are of a much higher frequency than those in the uncorrected data. Consequently, these variations would be more easily

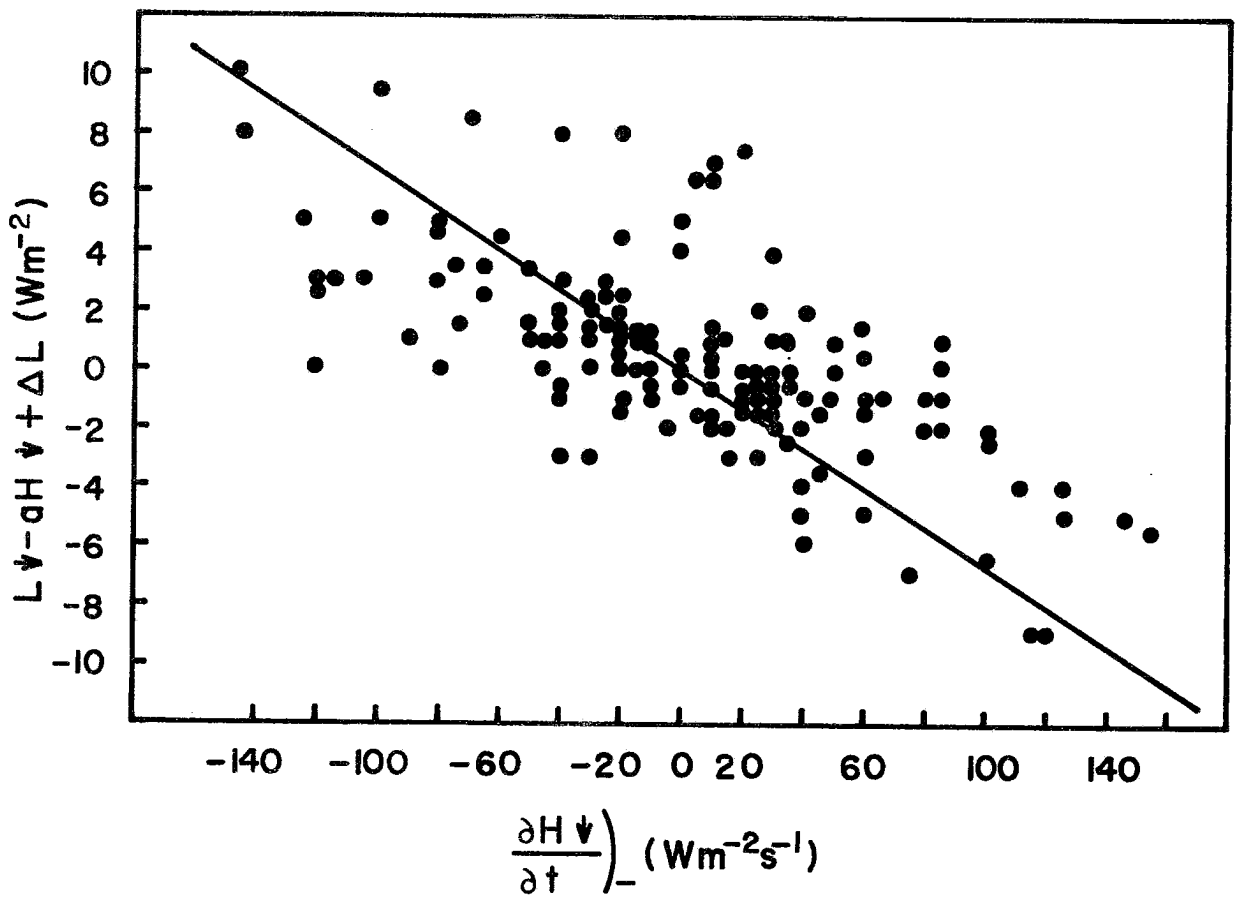

Figure 19. A plot of $L\downarrow_{meas} - aH\downarrow + n$ as a function of $\left.\frac{\partial H\downarrow}{\partial t}\right)_{-}$ for the 1301-1308 time period.

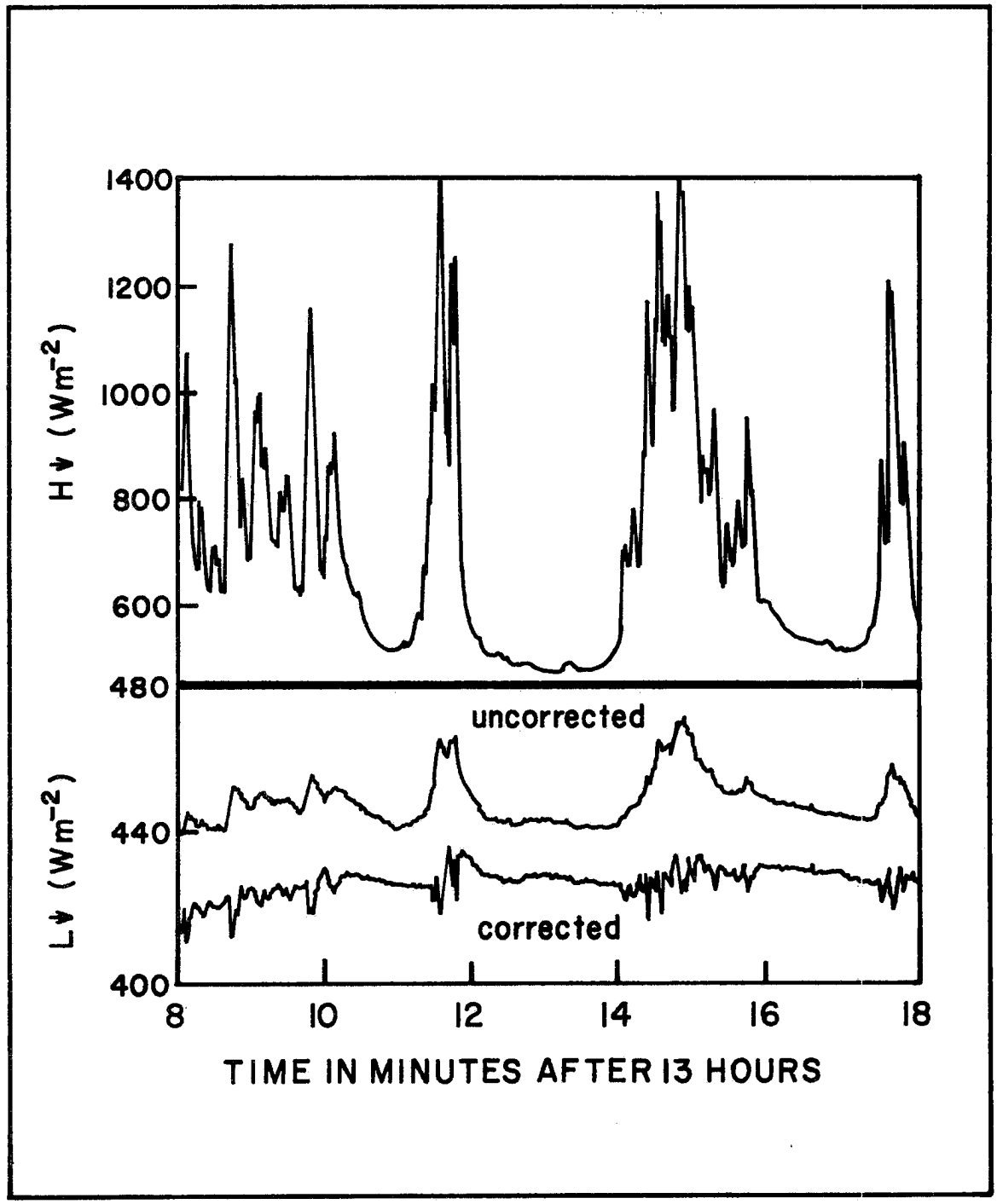

Figure 20. A comparison of corrected and uncorrected L↓ for the September 7, 1974, DC-6 flight.

filtered from the data than the variations which appear in the uncorrected data.

It should be noted that the empirical correction given here has been determined for a limited data set for a particular aircraft. The results are probably not general for other aircraft and should be examined carefully when applied to other GATE DC-6 data. However, in spite of the rather subjective analysis given here the feasibility of using an empirical correction for the direct solar heating of an aircraft mounted pyrgeometer has been clearly demonstrated.

VI. Conclusions

The actual performance of an Eppley pyrgeometer is compared to the desired theoretical performance. Several systematic errors are identified and evaluated in detail. The three most significant errors are shown to be due to (1) battery voltage uncertainties (2) non-linearity of circuitry at extreme temperatures and (3) differential heating of the instrument. The elimination of the error due to differential heating is shown to be essential to the successful calibration of the instrument.

Pyrgeometer measurements made from aircraft are shown to have errors as large as 50 Wm^{-2}. These errors, however, do not significantly affect the net radiation provided the upward and downward facing pyrgeometers are at the same equlibrium temperature and may be largely eliminated by making accurate measurements of the KRS-5 filter and the cold junctions of the thermopile. The corrections derived in this paper not only reduce the absolute errors, but significantly decrease the transient response of the instrument. The feasibility of using an empirical expression to correct errors due to solar heating is also demonstrated for aircraft measurements.

Although the specific applications discussed in this paper are directed toward aircraft measurements, the general results may be relevant to other applications of this instrument. The results should at the least serve as a guide to indicate the degree of instrumental sophistication needed in order to obtain a certain accuracy with the Eppley pyrgeometer.

ACKNOWLEDGEMENTS

We gratefully acknowledge the cooperation and support of the NCAR Research Aviation Facility and the NOAA Research Flight Facility in the airborne measurement portion of this research. The data reduction and analysis phases of this work have been supported by the Eppley Laboratories, the National Science Foundation, Climate Dynamics section, and the NOAA GATE Project Office.

REFERENCES

Albrecht, B., M. Poellot, and S.K. Cox, 1974: Pyrgeometer Measurements from Aircraft. Rev. Sci. Instrum., 45, No. 1, pp. 33-38.

Cox, S.K., 1973: Infrared Heating Calculations with a Water Vapor Pressure Broadened Continuum. Q.J. Roy. Meteor. Soc. , 99, No. 422, pp. 669-679.

Drummond, A.J., W.J. Scholes and J.H. Brown, 1970: A New Approach to the Measurement of Terrestrial Longwave Radiation. WMO Tech. Note No. 104, pp. 383-387.

Enz, J.W., J.C. Klink, and D.G. Baker, 1975: Solar Radiation Effects on Pyrgeometer Performance. J. Appl. Meteor., 14, pp. 1297-1302.

Faraponova, G.P., 1971: Tests of Radiation Thermoelements for Radiation Flux Measurements in the Atmosphere. Proceedings of the Sixth International Symposium on Actinometry and Atmospheric Optics, June 1966, Tartu, pp. 193-203.

Faraponova, G.P., and R.G. Timanovskaya, 1971: Field Tests of Radiation Thermoelements. Proceedings of the Sixth International Symposium on Actinometry and Atmospheric Optics, June 1966, Tartu, pp. 204-210.

Kozyrev, B.P., 1971: A Compensated Thermoelectric Net Radiometer with Whitened and Bright Detecting Surfaces Protected from Air Currents by KRS-5 Hemispheres. Proceedings of the Sixth International Symposium on Actinometry and Atmospheric Optics, June 1966, Tartu, pp. 168-176.

APPENDIX A

PYRGEOMETER MEASUREMENTS FROM AIRCRAFT

by

Bruce Albrecht

Michael Poellot

Stephen K. Cox

Department of Atmospheric Science

Colorado State University

Fort Collins, Colorado 80523

Pyrgeometer measurements from aircraft

Bruce Albrecht, Michael Poellot, and Stephen K. Cox

Department of Atmospheric Science, Colorado State University, Fort Collins, Colorado 80521
(Received 30 May 1973; and in final form, 14 September 1973)

An Eppley Laboratory pyrgeometer was tested in several different modes of operation to determine its ability to measure infrared irradiance from an aircraft platform. During the initial tests, the instrument output varied by 30–40 W m $^{-2}$ as the incident solar irradiance or air flow over the KRS-5 dome changed. The long pass filter (the KRS-5 dome) was found to be opaque to radiation of wavelengths shorter than 3.6 μ. Hence, the fluctuations described above may be attributed to changes in the temperature of the filter. The pyrgeometer output was studied as a function of the incident infrared irradiance and the temperature difference between the sensor surface and the KRS-5 dome. Laboratory tests verified this dependence and showed that by utilizing the thermopile cold junction and dome temperatures, infrared irradiances may be measured with a precision of $\pm$ 1.7 W m^{-2}. Although not the original intent of this research, it is shown that the KRS-5 shielded pyranometer may be used to measure infrared irradiance with a precision of $\pm$ 2 W m^{-2} in a ground station installation. However, in order to realize the precision value mentioned above, two precautions must be taken. First, the temperature of the KRS-5 dome must be monitored; and second, the entire instrument should have sufficient air flow over it to minimize temperature differences between the KRS-5 dome and the thermopile cold junction. The pyrgeometer was also mounted in an upward-looking configuration on an aircraft platform and measurements were made at constant pressure levels under clear sky conditions to approximate a constant irradiance. It was found that the intense flow over the instrument minimized the effect of the solar heating of the dome. Infrared irradiances measured on a day/night flight comparison differed by an average difference of 3.5 W m^{-2}, rms deviations about the mean value at any level were less than $\pm$ 2.5 W m^{-2}. Observed downward irradiance divergences differed from values calculated using a radiative transfer model by less than 0.3 W m^{-2} mb^{-1}. The ventilation, however, did not eliminate the sink–dome temperature differences because the temperature response of the thermopile heat sink is an order of magnitude slower than that of the KRS-5 dome; therefore, horizontal fluctuations of air temperature or abrupt changes of altitude result in erroneous output values. An attempt was made to determine an empirical correction for air temperature fluctuations from the aircraft air temperature data. No general correction factor relating temperature and output changes could be determined. However, individual applications of such an empirical relationship did reduce rms deviations of the output to less than 2 W m^{-2}.

I. INTRODUCTION

The Eppley Laboratory pyrgeometer[1] is an instrument intended to measure hemispheric infrared radiation in the spectral range of terrestrial radiation (4–100 μ). The instrument consists basically of a blackened thermopile enveloped by a hemisphere of KRS-5 with an interference filter vacuum deposited on the inside of the hemisphere (see Fig. 1).

The Eppley Laboratory pyrgeometer was tested in several different modes of operation to determine its limitations in measuring infrared irradiances, particularly from an aircraft instrument platform. These tests were conducted for both field and laboratory conditions. Similar instruments have been tested and described by Faraponova,[2] Faraponova and Timanovskaya,[3] and Kozyrev.[4]

In the initial tests, it was observed that the instrument responded to changes in incident solar radiation and changes in the air flow over the KRS-5 hemisphere. These observations were first made while monitoring the pyrgeometer output during a partly cloudy day and further confirmed by shading the instrument from the sun. The dependence on the air flow was demonstrated by forcing air over the KRS-5 dome during a sunny, cloud-free, day. By either shading the dome from the direct sun or by increasing the air flow, it was possible to change easily the output of the instrument by 0.21–0.29 mV, which corresponds to changes in irradiance of 30–40 W m^{-2}.

In an attempt to describe the dependence of the pyrgeometer on solar radiation, a measurement of the KRS-5 transmissivity was made. As can be seen from the results of this measurement (Fig. 2), there is virtually no transmittance of radiation whose wavelength is less than 3.6 μ (2800 cm^{-1}). Since only approximately 1.25% of the solar radiation has wavelength greater than 3.6 μ, one would expect less than 2 W m^{-2} solar radiation to be transmitted directly by the KRS-5 dome.

The reflective characteristics of the long pass filter (consisting of the KRS-5 hemisphere and the interference filter) were not determined. However, in the region where energy is transmitted by pure KRS-5, approximately 75% of the transmission loss is due to reflection.[5] Hypothetically, one may argue that even if the normal incidence reflectivity was as high as 90% at wavelengths where the material is totally opaque, as much as 50 W m^{-2} would be absorbed by the dome. If this heat were to be dissipated entirely by molecular diffusion, a temperature gradient of 20°C cm^{-1} would be necessary in the air surrounding the hemisphere.

Since the KRS-5 filter is opaque to radiation of wavelengths less than 3.6 μ, the fluctuations in the pyrgeometer output described above appear to be related entirely to

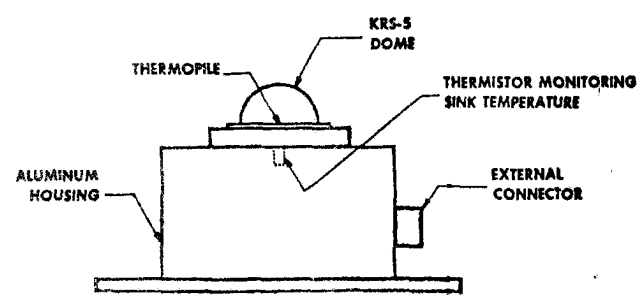

FIG. 1. Schematic depiction of the Eppley pyrgeometer.

© 1974 by the American Institute of Physics

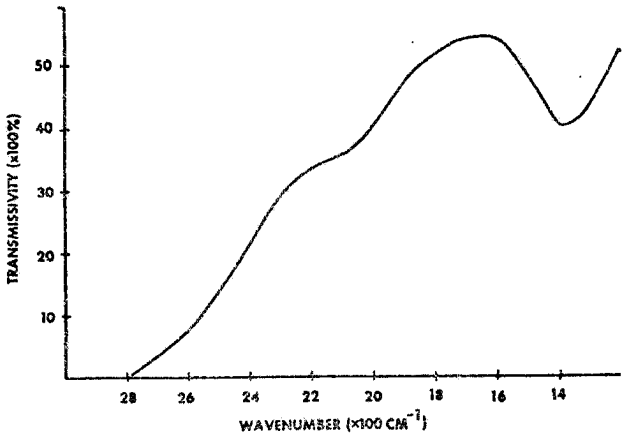

FIG. 2. Measured spectral transmissivity of KRS-5 dome (energy incident upon the outside of the dome).

changes in the filter's temperature. The mathematical and experimental results presented below quantify this dependence and indicate that accurate measurements of infrared irradiance may be made if the filter temperature is known.

Theoretically, the measurement of the incident radiation on the pyrgeometer sensor depends on the ability to accurately describe the heat budget of the sensor. In the configuration used by Eppley Laboratories, the thermopile output is an indication of the net radiation on the receiver surface, where[1]

$$R_{\text{net}}=(R_{\text{in}}-R_{\text{out}}). \tag{1}$$

Describing the components of R_{in} we have

$$R_{\text{in}}=\underbrace{H\tau(\downarrow)}_{A}+\underbrace{\epsilon_0\rho(\uparrow)\sigma T_S^4}_{B}+\underbrace{\epsilon(\uparrow)\sigma T_D^4}_{C}, \tag{2}$$

where T_S is the temperature of the sensor, T_D is the temperature of the KRS-5 dome, σ is the Stefan–Boltzmann constant, $\rho(\uparrow)$ is the reflectivity of the inside of the dome, and $\epsilon(\uparrow)$ is the emissivity of the same surface. $\tau(\downarrow)$ is the transmissivity and H is the irradiance on the dome. ϵ_0 is the emissivity of the sensor surface (assumed to be ~ 1). Term A in Eq. (2) represents the radiant power transmitted by the dome to the thermopile surface; term B is the portion of the radiant power emitted from the sensor and reflected back to the sensor surface by the inside of the dome; and term C represents the radiant power emitted from the KRS-5 dome to the sensor surface

$$R_{\text{out}}=\epsilon_0\sigma T_S^4 \tag{3}$$

Equation (3) represents the loss of radiant power by emission from the thermopile surface. Substituting Eqs. (2) and (3) into Eq. (1) and solving for H we obtain

$$H=\frac{R_{\text{net}}+\epsilon_0[1-\rho(\uparrow)]\sigma T_S^4-\epsilon(\uparrow)\sigma T_D^4}{\tau(\downarrow)}. \tag{4}$$

Rearranging terms, we have

$$H=\frac{R_{\text{net}}}{\tau(\downarrow)}+\frac{\epsilon_0[1-\rho(\uparrow)-\epsilon(\uparrow)]\sigma T_S^4-\epsilon(\uparrow)\sigma(T_D^4-T_S^4)}{\tau(\downarrow)} \tag{5}$$

if $\epsilon_0\sim 1$. But,

$$[1-\rho(\uparrow)-\epsilon(\uparrow)]=\tau(\uparrow), \tag{6}$$

where $\tau(\uparrow)$ is the transmissivity defined as the ratio of the energy transmitted through the dome to that incident upon the inside surface of the dome. It does not necessarily equal $\tau(\downarrow)$ since the long pass filter consists of two separate media—the KRS-5 dome and the interference filter deposited on the inside of the dome. The spectral $\tau(\uparrow)$ was measured to be significantly less than the spectral $\tau(\downarrow)$ at all wavelengths. From Eqs. (5) and (6),

$$H=\frac{R_{\text{net}}}{\tau(\downarrow)}+\frac{\epsilon_0\tau(\uparrow)}{\tau(\downarrow)}\sigma T_S^4-\frac{\epsilon(\uparrow)}{\tau(\downarrow)}\sigma(T_D^4-T_S^4). \tag{7}$$

In the above expression, conduction or convection heat transfer from the thermopile has been neglected. Hence, from this representation of the radiation budget of the sensor surface, one would expect that in order to make accurate measurements of the infrared irradiance H an accurate measurement of both T_S and T_D would have to be made.

It is useful to note that Eq. (7) may be expressed in terms of the thermopile cold junction (or thermopile sink) temperature, since the sensor temperature may be deduced if the cold junction temperature is known. The temperature of the thermopile sensor may be expressed as $T_S=T_C+\delta$, where T_C is the cold junction temperature and δ the temperature difference between the hot and cold junctions of the thermopile. For typical irradiance measurements in the atmosphere, δ has a maximum value of 0.5 K. Since $\delta\ll T_C$ (T_C approximately 200–300 K) Eq. (7) may be written as approximately

$$H=\frac{R_{\text{net}}}{\tau(\downarrow)}+\frac{\epsilon_0\tau(\uparrow)}{\tau(\downarrow)}\sigma T_C^4-\frac{\epsilon(\uparrow)}{\tau(\downarrow)}\sigma(T_D^4-T_C^4)+4\left(\frac{\epsilon_0\tau(\uparrow)}{\tau(\downarrow)}+\frac{\epsilon(\uparrow)}{\tau(\downarrow)}\right)\delta T_C^3, \tag{8}$$

where any terms involving products of δ have been ignored. Since δ is proportional to R_{net}, Eq. (8) may be written as

$$H=\frac{R_{\text{net}}}{\tau(\downarrow)}(1+KT_C^3)+\frac{\epsilon_0\tau(\uparrow)}{\tau(\downarrow)}\sigma T_C^4-\frac{\epsilon(\uparrow)}{\tau(\downarrow)}\sigma(T_D^4-T_C^4), \tag{9}$$

where K is a constant.

II. LABORATORY TESTS

During the manufacturer's calibration of the instrument, the temperature of the dome and the thermopile sink are maintained at the same temperature. This reduces Eq. (9) to

$$H=\frac{R_{\text{net}}}{\tau(\downarrow)}(1+KT_C^3)+\frac{\epsilon_0\tau(\uparrow)}{\tau(\downarrow)}\sigma T_C^4, \tag{10}$$

where $[R_{\text{net}}/\tau(\downarrow)](1+KT_C^3)$ represents the temperature compensated thermopile output and the term $[\epsilon_0\tau(\uparrow)/\tau(\downarrow)]\times\sigma T_C^4$ is supplied by a battery-thermistor compensation circuit. Consequently, if Eq. (9) is valid, one may hypothe-

TABLE I. rms deviation of the points along the regression lines in Fig. 3.

Run	rms deviation (W m^{-2})
1 (⊙)	1.1
2 (⊡)	1.7
3 (△)	2.3
4 (⊗)	1.5
Avg.	1.7

size that the output of the pyrgeometer for a constant infrared source will differ from the actual value of H by the amount $[\epsilon(\uparrow)/\tau(\downarrow)]\sigma(T_D^4-T_C^4)$, if $T_D \neq T_C$.

The dependence of the instrument output on this term may be observed by heating the dome and allowing it to cool while being irradiated by an infrared source of known or constant output. By making accurate measurements of the dome and the sink temperatures during this dome cool-down period, one may correlate the term $(T_D^4-T_C^4)$ with the pyrgeometer output.

Results of such an experiment are shown in Fig. 3. Different runs, depicted by the different symbols in Fig. 3, correspond to slightly different infrared source temperatures. The correlations are excellent. A summary of the rms deviation of the points about the regression lines may be found in Table I.

The instrument was tested for orientation dependence. This was accomplished by irradiating the sensor with a constant infrared source while varying the orientation of the instrument with respect to the vertical. When the instrument attitude was changed from a vertical orientation (thermopile sensor perpendicular to the force of gravity) to an orientation 20° from the vertical, no variation in the instrument output was observed.

The pyrgeometer was also examined for pressure dependence. The instrument output was monitored as the KRS-5 dome and the pyrgeometer housing were evacuated while infrared irradiance incident on the sensor was maintained constant. During these tests, the instrument was repeatedly evacuated to an equivalent atmospheric pressure of 50 mb (exterior atmospheric pressure 850 mb) with only random fluctuations of 0.01 mV (1.5 W m^{-2}) occuring in the pyrgeometer output.

III. AIRCRAFT TESTS

A. Day–Night Comparison

When mounted on an aircraft platform, the air flow over the instrument is considerably greater than if the instrument were mounted on a stationary support. Consequently, it would be expected that the sink and dome would be more effectively maintained at nearly the same temperatures. Therefore, it is to be expected that some of the uncertainty due to temperature differences between T_D and T_C would be eliminated from the pyrgeometer output.

This effect is shown in Fig. 4, which is a comparison between a day and night flight path with the pyrgeometer in an upward-facing configuration. Infrared measurements were made during these flights by flying at constant pressure altitudes at various heights above the surface. The flights

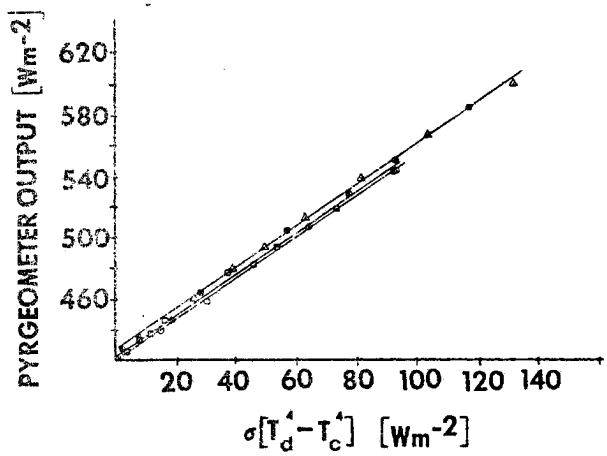

FIG. 3. Total pyrgeometer output as a function of the difference between dome and the thermopile sink temperature. The different symbols correspond to slightly different infrared source conditions.

were made under clear sky conditions with a minimum time of flight at any level of 8–10 min. The flights were made approximately 3 h apart flying identical flight paths.

These data indicate good agreement between the day and night flights. However, it should be noted that values obtained during the day flight tended to be slightly higher than those obtained after sunset. During the ground tests of the instrument, with no air flow over the dome, it was found as a crude approximation that the equivalent of 10% of the direct solar radiation is included in the pyrgeometer output. In the day flights, the average incident solar radiation was approximately 350 W m^{-2}. However, the average deviation between the day and night flights was only 4.1 W m^{-2}.

In a similar pair of profile flights, no solar loading was present in either flight; these flights were made at night with about 2 h between flights, and the results are summarized in Fig. 5. Again there is a good correlation between the values obtained during these flights, with an average deviation of about 3.5 W m^{-2}. It is important to note that in the four flights described above, at any level the average rms deviation of the measured downward irradiance from the mean value is 1.6 W m^{-2}, with a maximum deviation of 2.5 W m^{-2}.

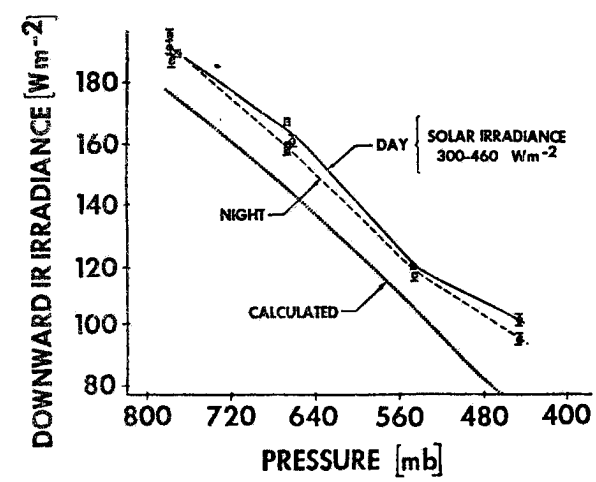

FIG. 4. Measured and calculated downward infrared irradiance for day (14:00 LST) and night (16:30 LST) flights of January 3, 1973.

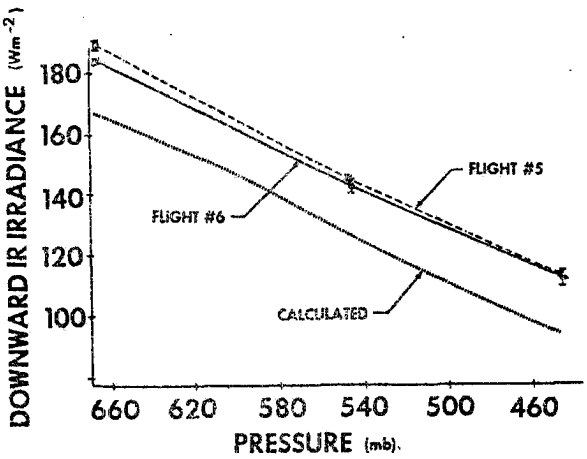

FIG. 5. Measured and calculated downward infrared irradiance for two night flights, flight 5 (16:00 LST) and flight 6 (18:00 LST) of December 19, 1972.

The above results, although obtained under somewhat uncontrolled infrared target conditions, indicate that the dependence of the instrument on solar radiation is significantly reduced when the instrument is mounted on the aircraft, particularly if the entire instrument is mounted in the slipstream of the aircraft.

B. Comparison with Calculated Infrared Divergence

An indication of the ability of the pyrgeometer to measure downward fluxes may be found by comparing the irradiances measured during the profile flights described above to irradiance values calculated by using a radiative transfer model.[6] Moisture, temperature, and pressure variables necessary for the calculations were obtained from both radiosonde and aircraft data. Temperature and humidity values at heights above where actual data were measured were obtained from U. S. *Standard Atmosphere Supplements, 1966*,[7] for January, 45°N latitude. O_3 values necessary for the calculations were obtained from a midlatitude ozone model portrayed in the same publication.

A comparison of the calculated values to those actually measured is made in Figs. 4 and 5. Although the magnitude of the calculated values is in all instances less than those measured, it is important to note the similarity of the slopes of these curves. The downward flux divergences of the calculated and the measured values are listed in Table II.

C. Temperature Lag of the Instrument

Although the air flow over the instrument on the aircraft seems to minimize the difference between sink and dome temperatures, the inherent dependence of the pyrgeometer output on these variables does impose some limitations on the usefulness of the unmodified instrument in this mode of operation. One of the problems is dependence of the instrument output on both sink and dome temperatures and their time response characteristics; this necessarily imposes a certain time response for the instrument to come into thermal equilibrium.

This time response is actually characterized by three independent physical characteristics of the instrument. The thermopile output has a response ($1/e$) given by Eppley Laboratories as approximately 2 sec. A response of this order was observed in the laboratory. The dome, on the other hand, requires about 4 to 5 min to come into thermal equilibrium with its environment. The thermopile sink, having a much larger mass than the dome, requires about 45–60 min to reach equilibrium.

When mounted on the exterior of an aircraft, the air flow over the instrument is considerably enhanced. Consequently, the response time of the instrument to various temperature variations is reduced. It is estimated that in the configuration used in the flight testing program, the time required for the dome to come into equilibrium is on the order of seconds, whereas the time required for the sink to reach equilibrium temperatures will be several minutes.

An immediate consequence of this response time difference is noticed by studying the output of the instrument under actual flight conditions. Figure 6 presents data collected from a profile flight as described above. The air temperature during this descent increased from −16°C to −6°C. Since the dome will respond much more quickly to the temperature change than will the sink, the dome will be at a warmer temperature. Consequently, the pyrgeometer will indicate a greater infrared value than actually exists by the amount of $[\epsilon(\uparrow)/\tau(\downarrow)]\sigma(T_D^4-T_C^4)$. As the aircraft continues at this constant height, it may be seen that the output eventually stabilizes as the sink reaches some equilibrium temperature (point C, Fig. 6). As seen from Fig. 6, the time required for a stabilization of the pyrgeometer output is on the order of several minutes.

Evidence that the thermopile sink temperature is increasing during the portion of the flight portrayed between points B and C in Fig. 6 may be readily obtained by measuring the thermopile output. The output of the radiation compensation circuit may be deduced from the difference between the total pyrgeometer output and the thermopile output, where the output of the radiation compensation circuit is proportional to T_C^4. Hence, in the B-C portion of the flight, it is seen that the difference between the thermopile output and the total output is increasing, indicating an increase in the temperature of the sink.

A corresponding instrument response is observed during the ascending mode of the profile flights. Figure 7 depicts

TABLE II. Comparison of measured and calculated values of flux divergence.

Flights 5 and 6		
Pressure layer (mb)	Flux divergence (W m^{-2} mb^{-1}) Measured	Calculated
546–667	0.362	0.334
447–546	0.310	0.338
Flight 10		
Pressure layer (mb)	Flux divergence (W m^{-2} mb^{-1}) Measured	Calculated
778–667	0.296	0.285
667–546	0.340	0.334
546–446	0.223	0.321

an ascent from 550 mb to 450 mb, where the temperature has decreased from −16°C to −28°C (point A to point B on Fig. 7). When the aircraft levels off at 450 mb, the output of the pyrgeometer is lower than the equilibrium values obtained after point C on Fig. 7. This type of response would be expected, since at point B the dome will have a colder temperature than the sink.

A similar complication due to the differential temperature response of the various parts of the instrument is observed on the profile flights after the entire instrument is assumed to have reached thermal equilibrium. In this case, it was noted that the instrument output indicated fluctuations corresponding to small variations in the air temperature. Here it is felt that the dome responded quickly to these small fluctuations in temperature while the temperature of the sink remained virtually unaffected.

D. Statistical Analysis of Temperature Dependence

If the pyrgeometer output were affected by small fluctuations in air temperature, it is possible that an empirical relationship between the output and the fluctuations could be established. To investigate this possibility, nine flight legs were selected for analysis, assuming a constant irradiance for the duration of each leg. The data sampling rate was one per second.

Three data legs were selected from a flight in which the instrument was mounted in a downward-looking configuration. Passes were made at approximately 15, 46, and 76 m above a snow-covered reservoir, each pass lasting about 1 min. Since the surface air temperature that day was 5.1°C, the target area was assumed to be uniform at an equivalent blackbody temperature of 0°C, which was verified with a Barnes PRT-5 radiometer mounted on the bottom of the aircraft.

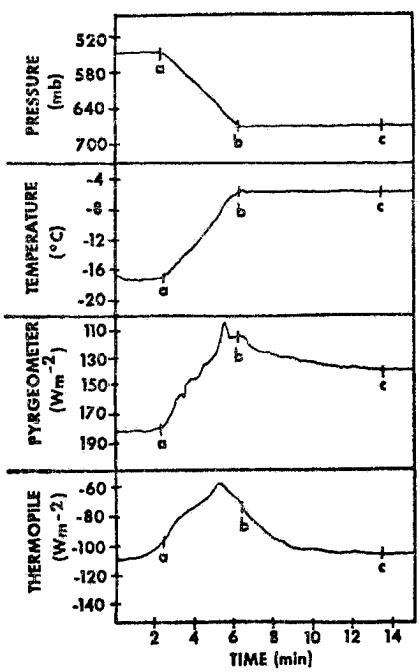

FIG. 6. Example of data illustrating temperature response during descent.

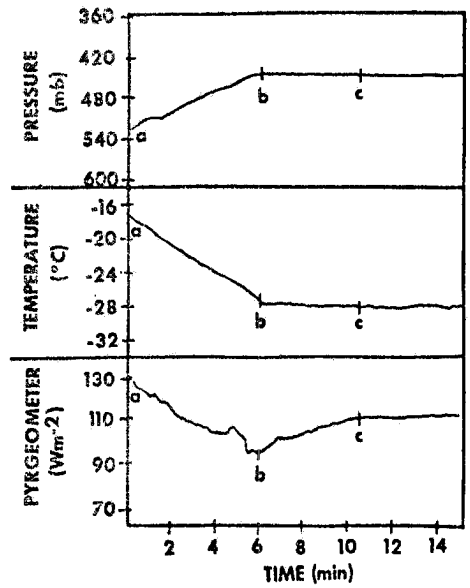

FIG. 7. Example of data illustrating temperature response during ascent.

On the other six data segments, the pyrgeometer was mounted in an upward-looking configuration. These data were collected at constant pressure altitudes at night under clear sky conditions. Each level was maintained for 10 min, but only the last 3–5 min were analyzed, to ensure that the sink had reached equilibrium temperature.

Although it has been determined in Sec. II that output fluctuations should be proportional to $(T_D^4-T_C^4)$, the curve of T^4 may be considered linear for a small range of temperature. This allows the following assumption to be made for each leg:

$$H'=\bar{H}+k(T'-\bar{T}), \tag{11}$$

where H' and T' are individual data samples for the pyrgeometer output and temperature, $\bar{H}$ and $\bar{T}$ are mean values for the sample leg, and k is the empirical constant to be determined. It is assumed here that $\bar{T}$ is identical to the sink temperature and H is the constant irradiance value. $\bar{T}$ was measured with a reverse flow temperature sensor mounted on the wing of the aircraft.

In order to account for the response time of both the pyrgeometer and the temperature sensor, a time lag of 4 sec was determined graphically from the data, assuming a direct correlation between the air temperature and instrument output. This makes the analytical expression

$$H_t'=\bar{H}+k(T_{t-4}'-\bar{T})=\bar{H}+k\Delta T. \tag{12}$$

Thus, a plot of H' vs ΔT should approximate a straight line of slope k.

To find the best fit to the data, a least squares linear regression was performed from which k and an rms deviation about the line were calculated. rms deviations about the mean for both the pyrgeometer output and temperature were also determined for each leg. The results of these calculations are summarized in Table III.

This table indicates that, although there is a general correlation between temperature and pyrgeometer output

TABLE III. Summary of statistical analysis of aircraft data.

Flight level[a]	$\bar{H}$ (W m^{-2})	$\bar{T}$ (K)	Number of values	k (W m^{-2} K^{-1})	H' rms deviation about line (W m^{-2})	H' rms deviation about mean (W m^{-2})	T' rms deviation about mean (K)
Downward-looking configuration							
15 m	321.7	279.1	58	10.0	1.0	4.2	0.40
46 m	330.8	280.4	57	6.4	1.5	6.5	0.55
76 m	332.2	280.2	64	3.6	0.98	5.3	0.38
Upward-looking configuration							
776 mb ↑	187.7	273.3	295	5.0	2.0	2.2	0.18
779 mb ↓	192.6	273.5	295	4.5	0.98	1.3	0.12
667 mb ↑	157.0	267.5	295	0.2	1.1	1.3	0.12
668 mb ↓	158.4	267.2	175	−8.5	0.66	1.1	0.05
547 mb ↓	118.3	256.6	235	−2.0	0.56	0.94	0.28
446 mb ↑	94.6	245.5	235	−1.1	4.6	4.7	0.14

[a] Arrow indicates aircraft ascent ↑ or descent ↓ to level.

fluctuations, a linear empirical relationship between temperature and pyrgeometer error is not sufficient to correct the instrument output. Values of k differed between legs by as much as an order of magnitude and even showed negative correlations at higher altitudes, and these differences could not be related to rms deviations in either output or temperature.

A significant result of this analysis is that the application of the empirical relationship reduced the average rms deviation of the pyrgeometer output by more than a factor of 2. Assuming a constant source, this scatter represents the noise of the output, and the reduction of this noise indicates a dependence of the output on temperature fluctuations.

This analysis confirms that the pyrgeometer measurements may be corrected for the KRS-5 dome–sink temperature difference. In future applications of the pyrgeometer, a direct measurement of the KRS-5 dome temperature is highly desirable.

ACKNOWLEDGMENTS

The contributions of many individuals in the NCAR Research Flight Facility made the flight test portion of this research possible. We gratefully acknowledge their cooperation and support. The authors also wish to thank Dr. J. DeLuisi, Dr. M. O'Donnel, and Dr. P. Crooimans for their advice and assistance during various phases of this research. This research has been funded by the Atmospheric Science Section, National Science Foundation, NSF Grant No. GA-36302.

[1] "Instrumentation for the Measurement of the Components of Solar and Terrestrial Radiation" (Eppley Laboratory Inc., Newport, R. I., 1971).
[2] G. P. Faraponova, "Tests of Radiation Thermoelements for Radiation Flux Measurements in the Atmosphere," *Proceedings of the Sixth International Symposium on Actinometry and Atmospheric Optics, June 1966, Tartu*, edited by V. K. Pyldmaa (Israel Program for Scientific Translations, Jerusalem, 1971), pp. 193–203.
[3] G. P. Faraponova and R. G. Timanovskaya, "Field Tests of Radiation Thermoelements," in Ref. 2, pp. 204–210.
[4] B. P. Kozyrev, "A Compensated Thermoelectric Net Radiometer with Whitened and Bright Detecting Surfaces Protected from Air Currents by KRS-5 Hemispheres," in Ref. 2, pp. 168–176.
[5] R. A. Smith, F. E. Jones, and R. P. Chasmar, *The Detection and Measurement of Infrared Radiation* (Oxford U. P., London, 1968), p. 361.
[6] S. K. Cox, Quart. J. R. Met. Soc. 99, 669 (1973).
[7] United States Committee on Extension to the Standard Atmosphere, *U. S. Standard Atmosphere Supplements*, (U.S. GPO Washington, D. C., 1966), pp. 12–13, 78–80, 111–113.

BIBLIOGRAPHIC DATA SHEET	1. Report No. CSU-ATSP-251	2.	3. Recipient's Accession No.
4. Title and Subtitle Pyrgeometer Data Reduction and Calibration Procedures			5. Report Date May 1976 6.
7. Author(s) Bruce Albrecht and Stephen Cox			8. Performing Organization Rept. No. CSU-ATSP-251
9. Performing Organization Name and Address Department of Atmospheric Science Foothills Campus Colorado State University Fort Collins, Colorado 80523			10. Project/Task/Work Unit No. 11. Contract/Grant No. NSF OCD 74-21678
12. Sponsoring Organization Name and Address Eppley Laboratories - Newport, Rhode Island National Science Foundation - Washington, D. C. NOAA GATE Project Office - Rockville, Maryland			13. Type of Report & Period Covered 14.

15. Supplementary Notes

16. Abstracts

The actual performance of an Eppley pyrgeometer is compared to the desired theoretical performance. Several systematic errors are identified and evaluated in detail. The three most significant errors identified are due to (1) battery voltage uncertainties (2) non-linearity of circuitry at extreme temperature and (3) differential heating of the instrument. The elimination of the error due to differential heating is found to be essential to the successful calibration of the instrument. A pyrgeometer laboratory calibration technique is described.

Pyrgeometer measurements made from aircraft are shown to have potential errors as large as 50 Wm^{-2}. These errors, however, do not significantly affect the net radiation provided the upward and downward facing pyrgeometers are at the same equilibrium temperature, and may be largely eliminated by making accurate temperature measurements of the KRS-5 dome and the cold junctions of the thermopile. The corrections considered in this paper not only reduce the absolute errors but significantly decrease the transient response of the instrument. The feasibility of using an empirical expression to correct errors due to solar heating is also demonstrated for aircraft measurements.

17. Key Words and Document Analysis. 17a. Descriptors

Infrared Observations

Pyrgeometer

17b. Identifiers/Open-Ended Terms

17c. COSATI Field/Group

18. Availability Statement	19. Security Class (This Report) UNCLASSIFIED	21. No. of Pages 55
	20. Security Class (This Page UNCLASSIFIED	22. Price

FORM NTIS-35 (REV. 3-72) THIS FORM MAY BE REPRODUCED USCOMM-DC 14952-P72